

Quark combinatorics and meson production ratios in hadronic Z^0 decays

V. V. Anisovich, V. A. Nikonov

Petersburg Nuclear Physics Institute, Gatchina, 188300 Russia

and J. Nyiri

Research Institute for Particle and Nuclear Physics, Budapest, Hungary

(August 14, 2000)

Rich experimental data accumulated in the past few years in the hadronic Z^0 decays allow one to check the quark combinatorics relations for a new type of processes, namely: quark jets in the decays $Z^0 \rightarrow q\bar{q} \rightarrow \text{hadrons}$. In this paper we review quark combinatorics rules for the yields of vector and pseudoscalar mesons, V/P , in the central and fragmentation regions of the hadronic Z^0 decays. It is stressed that in the central region a direct verification of quark combinatorics rules is rather problematic because of a considerable background related to the decay of highly excited resonances; however such a verification is possible in the fragmentation region, at $x_{\text{hadron}} \sim 0.5 - 1$, where the contribution of resonance decays is suppressed due to the rapid decrease of spectra with increasing x_{hadron} . It is shown that the experimental data in the fragmentation region for ρ^0/π^0 and p/π^+ are in a reasonable agreement with the predictions of quark combinatorics. The ratios of the heavy meson yields, B^*/B and D^*/D , are also discussed: the data demonstrate a good agreement with the quark combinatorial results. We analyse the structure of the suppression parameters for strange and heavy quark productions in soft processes and estimate their order of magnitudes in the multiperipheral processes; the ratio K^\pm/π^\pm at $x_{\text{hadron}} \sim 0.5 - 0.8$ and production probabilities of the $c\bar{c}$ and $b\bar{b}$ mesons are in a good agreement with the estimates.

I. INTRODUCTION

The relations of quark combinatorics for hadron yields were originally based on the qualitative treatment of a multiparticle production process as a process of production of a "cloud" of non-correlated quarks and antiquarks followed by their occasional fusion into mesons and baryons [1,2]. In this picture the quark combinatorics approach echoes the statistical treatment of reactions of nucleus decays [3], and actually it was initiated by the success of the statistical methods in the description of multinucleon processes. There is one more common point in treating multinucleon and multi-quark processes: the stage of final state interactions. In multinucleon reactions the Watson–Migdal factor [4] leads to an increase of the low-energy contributions in the nucleon–nucleon final state interactions. In multi-quark reactions the analogous effect of the $q\bar{q}$ and qqq final state interactions, as one can guess, should enlarge the production of the comparatively low-mass mesons and baryons: in [5] a hypothesis was made about the dominant contribution of several low-mass $q\bar{q}$ and qqq multiplets to the spectra of produced hadrons.

This particular story reflects a general trend of how methods and approaches used in nuclear physics influenced the physics of strong interactions. But, as time goes on, our understanding of QCD, the theory of strong interactions, becomes deeper, and now a new level of understanding of quark-gluon physics in the soft interaction region forces us to review the relations of quark combinatorics.

a) Quark combinatorics for hadron production.

The rules of quark combinatorics, as it was stressed above, were initially suggested for finding probabilities of hadron yields in the multiparticle production processes [1,2]. Later, they were extended to meson decay processes, see [6]. In [1,2] (see also [5]) the hadronic production processes were treated on the basis of the following qualitative picture. In the multiparticle production process there is a stage of a cloud of constituent quarks. When joining each other, they create mesons ($q\bar{q}$), baryons (qqq) and antibaryons ($\bar{q}\bar{q}\bar{q}$). The probabilities to form hadrons of different sorts are defined by combinatorial rules which have been obtained under the assumption that quarks and antiquarks of the sea are produced uncorrelated and there is neither spin nor isospin alignment.

Our knowledge of the multiparticle production mechanism, i.e. the structure of amplitudes responsible for the inclusive production, is now, however, more complete, thus allowing us to investigate the basis of quark combinatorics at a new level. In the present paper, we investigate

- (i) the ratio of vector/pseudoscalar meson yields both for the central and fragmentation regions of the quark jets in the hadronic Z^0 decays (Sections 2 and 3, respectively), and
- (ii) the structure of the suppression parameters for production of strange and heavy quarks in the multiperipheral processes (Section 4).

Time is ripe for this review, for in the meantime quark combinatorics has become widely used for the consideration of meson resonances with masses 1.0-2.5 GeV, with a goal to determine the quark-gluon content of these states by investigating the transitions *resonance* \rightarrow *mesons* [7–9]. In the investigation of exclusive decay processes [7–9], the qualitative picture of the cloud structure of sea quarks is not used (that makes the conclusions more model-independent). However, the notion "suppression parameter" for the production of strange quarks plays an important role, and it is the same as what is used in multiparticle production processes. Thus, we have to re-think quark combinatorics on a new basis both theoretically and experimentally.

b) Hadronic Z^0 decays.

We discuss here the yields of vector ($\rho^0, \omega, \bar{K}^*$) and pseudoscalar (π, K) mesons in the hadronic Z^0 decay. Currently there exists rich experimental information on these processes, which are determined by transitions $Z^0 \rightarrow q\bar{q} \rightarrow$ *hadrons*. First, we consider the production of light-flavour mesons, which are created in the quark jets $Z^0 \rightarrow u\bar{u}$, $Z^0 \rightarrow d\bar{d}$, $Z^0 \rightarrow s\bar{s}$ with probabilities [10]:

$$u\bar{u} : d\bar{d} : s\bar{s} \simeq 0.26 : 0.37 : 0.37 \quad (1)$$

The large mass of the Z^0 boson makes it possible to observe in hadronic decays $Z^0 \rightarrow q\bar{q} \rightarrow$ *hadrons* the characteristic features of both multiparticle production (central region of quark jets) and meson decay processes (fragmentation production).

The data accumulated by the Collaborations ALEPH [11], L3 [12], DELPHI [13] and OPAL [14] provide spectra of vector and pseudoscalar mesons, $d\sigma/dx(Z^0 \rightarrow V + X)$ and $d\sigma/dx(Z^0 \rightarrow P + X)$ in a broad interval of x , thus giving an opportunity to compare them with the predictions of quark combinatorics.

c) Hadron production in the central region, and the vector-pseudoscalar ratio.

In Section 2 the hadron production in the central region in the quark jet is considered. We discuss the prompt vector meson (V) and pseudoscalar meson (P) yields. For particles belonging to the same $q\bar{q}$ multiplet we obtain:

$$\frac{V_{prompt}}{P_{prompt}} = 3. \quad (2)$$

This is a well-known result of the quark combinatorics [1,2,5] for hadron-hadron collisions. Hence, our analysis shows that the ratio V_{prompt}/P_{prompt} is the same for pomeron ladder in hadron-hadron collisions and for quark jets, despite of the different structure of the colour exchanges in these processes.

As we have already said, the rules of quark combinatorics for hadron-hadron collisions were introduced in [1,2,5]. Investigations of the QCD-pomeron [15,16] shed light on quark-gluon structure of the multiperipheral ladder in hadron collisions and allowed us to deal with meson yields in the central region on a new level. Therefore, in Appendix A we give a new analysis of the results of quark combinatorics for V_{prompt}/P_{prompt} at $x \sim 0$, using Lipatov's pomeron [16] as a guide.

d) Suppression of strange quark production.

An important feature in hadron production is the suppression of the production probability of the strange quark in the multiperipheral ladder:

$$u\bar{u} : d\bar{d} : s\bar{s} = 1 : 1 : \lambda, \quad (3)$$

with $0 \leq \lambda \leq 1$. This topic is discussed at Section 4: it is shown that $\lambda \simeq m^2/m_s^2$, where m and m_s are masses of non-strange and strange constituent quarks, respectively.

This suppression results in a suppression of the production of mesons containing strange quarks that is observed in the hadronic Z^0 decays.

e) Soft colour neutralisation of quarks in the hadronic Z^0 decay.

When considering central production at the decay $Z^0 \rightarrow q\bar{q} \rightarrow$ *hadrons* we start with the standard mechanism of soft colour neutralisation of the outgoing quarks: newly-born quark-antiquark pairs are produced in multiperipheral ladder (see Fig. 1a), which provides the transfer of the colour from antiquark to quark. The discontinuity of the self-energy diagram of Fig. 1b (determined by cutting through hadronic states, dashed line in Fig. 1b) defines the transition cross section $Z^0 \rightarrow$ *hadrons*, while the quark-gluon block inside the big quark loop determines the confinement forces.

Likewise, the inclusive production cross section of the meson in the central region is provided by the discontinuity of the diagram of Fig. 1c. The quark loop *meson* $\rightarrow q\bar{q} \rightarrow$ *meson* shown in Fig. 1c with the production of vector or pseudovector mesons determines relative probabilities of these particles. The chain of the quark loops shown on Figs. 1b, 1c and 1d (below we denote this chain as A) contains both colour singlet ($c = 1$) and colour octet ($c = 8$) components: $A = A_1 + A_8$. According to the rules of $1/N$ -expansion [17], the main contribution is due to the octet component. The idea that the quark leaves the confinement trap by a production of new quark-antiquark pairs is

rather old; it has been discussed long ago (for example, see [5], Sections 7 and 9, as well as [18]). A new impulse in understanding the confinement mechanism has been brought by Gribov [19]. Following the ideas of [19], we use the jet structure shown in Fig. 1a assuming that the t -channel exchange by quark is a constructive element of the jet.

Spectroscopic calculations (see, for example, [20]) support the hypothesis about the scalar type of confinement forces; accordingly, we assume that the chain A realises the t -channel exchange with $J^P = 0^+$.

The calculation of the block for central meson production performed in Section 2 proves that equation (2) is fulfilled, if the wave functions of mesons (V and P) belonging to the same multiplet are equal.

f) Prompt hadron production and production due to the decay of high resonances.

The equality (2) is valid for prompt meson production, while the decays of highly excited states violate this ratio as is seen in the experiment, providing the increase of the rate of light mesons due to resonance decay. As to ρ/π and K^*/K , the decays increase the contribution of pseudoscalar component. According to [11], $\rho^0/\pi^0 = 0.15 \pm 0.03$, and $K^*/K = 0.40 \pm 0.06$, that indicates on a large contribution into spectra from the decays of highly excited states.

The problem of the production and decay of highly excited states in hadron-hadron collisions had been discussed in [21]. The conclusion was similar: average multiplicities of the produced light mesons and baryons result mainly from the cascade decays of the highly excited resonances.

The multiperipheral structure of the ladder allows us to estimate the resonance masses which are important for meson production; they are of the order or less than 2 GeV (Section 5)

The existence of the decay of highly excited resonances is a reality that one should take into account in the verification of quark combinatorial rules. We discuss several ways of solving this problem.

g) Heavy meson production in $Z^0 \rightarrow b\bar{b}$ and $Z^0 \rightarrow c\bar{c}$ decays.

One way is to check quark combinatorics for heavy particle yields, where the cascade multiplication is suppressed. An ideal example could be the production of mesons containing a b -quark. In fact, for the beauty mesons the ratio B^*/B observed in the experiment agrees with (2). When the lowest S -wave multiplet dominates in the production of heavy mesons, then one has (provided the equation (2) is fulfilled): $B \simeq B_{prompt} + B_{prompt}^* = 4B_{prompt}$, and the ratio of vector and pseudoscalar mesons is $B^*/B \simeq 0.75$.

At the experiment on Z^0 decay it was observed: $B^*/B = 0.771 \pm 0.075$ [22], 0.72 ± 0.06 [23], 0.76 ± 0.10 [24], 0.76 ± 0.09 [25]; the mean value is 0.75 ± 0.04 .

For charmed mesons $D^*/D = 0.60 \pm 0.05$ [26], 0.62 ± 0.03 [27], 0.57 ± 0.05 [28]. The mean value is 0.61 ± 0.03 , which means a rise of the contribution from the decay of the non- S -wave multiplets.

One should stress that the ratios V/P for beauty and charmed mesons are saturated in the fragmentation region due to the transitions $Z^0 \rightarrow b\bar{b}$ and $Z^0 \rightarrow c\bar{c}$. Therefore, in Section 3 we re-analyse quark combinatorics for the fragmentation region of the hadronic Z^0 decay.

The production cross section of mesons in the fragmentation region is determined by the discontinuity of the diagram of Fig. 1c (the cutting of ladder diagram is shown by dashed line). Direct calculations demonstrate that (2) is fulfilled with rather good accuracy for the fragmentation region as well, provided the wave functions of vector and pseudoscalar mesons are equal.

h) Production of light-flavour mesons in the fragmentation region of the hadronic Z^0 decay.

Investigations of meson production in the fragmentation region open the way to test the rules of quark combinatorics for light-flavour hadrons, and to verify (2) in particular. As is said above, in the spectra of light-flavour hadrons the contribution of the component related to the decay of highly excited states dominates. Still, in the case of jet processes this component dominates in the central region, at $x \sim 0$, but not in the fragmentation one. The hadronic spectra for jets are maximal at $x \sim 0$, and they decrease rapidly with the growth of x . As a result, the component which comes from a resonance decay decreases quickly, because the decay products share the value $x_{resonance}$, thus entering the region of smaller x . In due course this effects a fast growth of relative contributions from prompt particle production. Therefore, the measurements of particle yields at $x \sim 0.5 - 1.0$ provide an opportunity for model-independent testing of quark combinatorics.

In Section 3 we compare the ratios ρ^0/π^0 and K^*/K measured in [11] at large x with quark combinatorics predictions; in Section 5 the baryon-meson ratio, p/π^+ , is discussed. comparison demonstrates reasonable agreement of the experimental data with the predictions of quark combinatorics.

i) Heavy quark production suppression.

Multiperipheral dynamics of the quark-gluon ladder in the processes of Fig. 1 results in a strong suppression of production of new heavy quark pairs, $Q\bar{Q}$. The suppression parameter (relative probability) is of the order of $\lambda_Q \simeq m^2/(m_Q^2 \ln^2(\Lambda^2/m_Q^2))$, where m_Q is the mass of heavy quark and Λ is the QCD scale parameter, $\Lambda \sim 200$ MeV. One has $\lambda_c \simeq 2.8 \cdot 10^{-3}$ and $\lambda_b \simeq 1.1 \cdot 10^{-4}$.

The inclusive production of the $c\bar{c}$ and $b\bar{b}$ mesons in Z^0 decays agrees with this estimation (Section 4).

j) The ratio ω/ρ^0 and interference of flavour amplitudes at $x \sim 1$.

The rules of quark combinatorics give us $\omega_{\text{prompt}}/\rho_{\text{prompt}}^0 = 1$. It can be proven that the decays of highly excited states effect weakly this equality. Indeed, the masses of ρ and ω are almost equal, so the phase spaces of the decay processes influence equally the probabilities of their yields. The experiment confirms this statement: at $x \sim 0.1 - 0.2$ the value $\omega/\rho^0 = 1$ is observed. However, at larger x the experimental value is $\omega/\rho^0 < 1$. This reveals the interference of flavour amplitudes. The fact is that the decay vertices for $Z^0 \rightarrow u\bar{u}$ and $Z^0 \rightarrow d\bar{d}$ have opposite signs, thus enhancing the coherent production of the ρ^0 meson and suppressing the production of ω (Section 6).

II. PROMPT PRODUCTION IN THE CENTRAL REGION OF THE QUARK JET: THE RATIO $V/P = 3$

In this Section we discuss the prompt production of vector and pseudoscalar mesons (for definiteness, ρ and π) in the central region of a quark jet. The production cross section is determined by the discontinuity of the diagram shown in Fig. 1c; it is re-drawn in Fig. 2a. A particular feature of the production of ρ and π is the presence of a loop diagram, which is shown separately by Fig. 2b. Below we calculate these loop diagrams for ρ and π using the spectral integration technique which is discussed in detail in [29,30]. Within this technique the loop diagrams are expressed in terms of the ρ and π light-cone wave functions.

But first, let us present the result of our calculations.

Direct calculations lead to the following formulae for the inclusive cross section of the ρ and π mesons at $x \sim 0$:

$$\begin{aligned} \frac{d\sigma}{dx}(Z^0 \rightarrow \rho + X) &= \frac{1}{16\pi^3} \int_0^1 \frac{d\xi}{\xi(1-\xi)} \int d^2\mathbf{k}_\perp \psi_\rho^2(\xi, \mathbf{k}_\perp) \cdot 3\Pi_Z(W_1^2, W_2^2) \\ \frac{d\sigma}{dx}(Z^0 \rightarrow \pi + X) &= \frac{1}{16\pi^3} \int_0^1 \frac{d\xi}{\xi(1-\xi)} \int d^2\mathbf{k}_\perp \psi_\pi^2(\xi, \mathbf{k}_\perp) \cdot \Pi_Z(W_1^2, W_2^2) . \end{aligned} \quad (4)$$

Here ψ_ρ and ψ_π are quark wave functions of ρ and π mesons, ξ and \mathbf{k}_\perp are quark light-cone variables (the fraction of momentum carried by a quark along the z -axis and its momentum in the (x, y) -plane, respectively). In (4) one can see explicit expressions related to the production of ρ and π mesons. The rest (contribution from the large quark loop as well as from ladder diagrams) is designated in (4) as $\Pi_Z(W_1^2, W_2^2)$, which depends on the invariant energies squared for the quark chains, W_1^2 and W_2^2 . Multiperipheral kinematics give:

$$W_1^2 W_2^2 \simeq \xi(1-\xi)(m^2 + k_\perp^2)M_Z^2 . \quad (5)$$

Here M_Z is the mass of the Z^0 boson.

The factor 3 in the ρ production cross section is the result of summing over polarizations of the vector particle.

Equation (4) directly demonstrates that, if quark wave functions of ρ and π are identical, that is assumed by the quark multiplet classification of these mesons, then at $x \sim 0$ we have $d\sigma(Z^0 \rightarrow \rho + X)/dx : d\sigma(Z^0 \rightarrow \pi + X)/dx = 3 : 1$. Let us stress again: the equation (4) as well as diagrams of Figs. 1c, 2a, 2b stand for promptly produced mesons.

A. Spectral representation for the loop diagram of Fig. 2a

The calculation of the diagram of Fig. 2a in terms of spectral integration is performed in the following steps (see also [29,30]):

- (i) quark loops in Fig. 2a are taken energy-off-shell;
- (ii) for the energy-off-shell quark loops the discontinuities are calculated (corresponding cuts are shown by the dotted lines I, II, III and IV);
- (iii) the spectral integrals are determined by the discontinuities being the integrands.

First, consider the double spectral integral which corresponds to the cuts III and IV, which are the spectral integrals over effective masses squared, M^2 and M'^2 , in the transitions $Z^0 \rightarrow q\bar{q}$ and $q\bar{q} \rightarrow Z^0$:

$$\begin{aligned} \int_{4m^2}^{\infty} \frac{dM^2 dM'^2}{\pi^2} \frac{g_Z(M^2)g_Z(M'^2)}{(M^2 - M_Z^2)(M'^2 - M_Z^2)} d\Phi(P_Z; p_1, p_2) d\Phi(P'_Z; p_3, p_4) \\ \times S_Z T(p; q_1, q_2) A(W_1^2, q_1^2) A(W_2^2, q_2^2) . \end{aligned} \quad (6)$$

Here $g_Z(M^2)$ is the vertex function for the $Z^0 \rightarrow q\bar{q}$ transition and M_Z is the Z^0 boson mass. The factors $d\Phi(P_Z; p_1, p_2)$ and $d\Phi(P'_Z; p_3, p_4)$ are phase spaces related to the cuts III and IV. S_Z is the spin factor for the big quark loop in Fig. 2a. The amplitudes $A(W_i^2, q_i^2)$, ($i = 1, 2$), refer to the quark-gluon chains with the t -channel scalar quantum numbers (see discussion in Section 1.e), and $T(p; q_1, q_2)$ is the block which corresponds to the small quark loop (the $q\bar{q}$ loop for production of ρ and π mesons).

The characteristic feature of the spectral integral (6) is the large value of M_Z . Because of that one can replace, with rather good accuracy, the poles of the spectral integrand by half-residues:

$$\frac{1}{M^2 - M_Z^2} \rightarrow -i\pi\delta(M^2 - M_Z^2), \quad \frac{1}{M'^2 - M_Z^2} \rightarrow i\pi\delta(M'^2 - M_Z^2). \quad (7)$$

Equation (6) stands for the discontinuity of the amplitude that results in different signs for the half-residues in (7). Equation (7) means that the block inside of the big quark loop can be considered, with a good accuracy, as a block of the real process. This is a well-known feature of the high-energy jets; below we use it for estimating meson production amplitudes.

We are not especially interested in the spectral integral (6) determined by the big quark loop, since it is quite common for the π and ρ production. Our target is the spectral integral which corresponds to the amplitude $T(p; q_1, q_2)$ that is the ρ or π meson production block. This block is shown separately in Fig. 2b.

B. Calculation of the loop diagram of Fig. 2b

The amplitude of the loop diagram of Fig. 2b represented as a double dispersion integral is:

$$M = T(p; q_1, q_2) 2p_0 (2\pi)^3 \delta^{(3)}(\mathbf{p} + \mathbf{q}_1 - \mathbf{q}_2 - \mathbf{p}'), \quad (8)$$

$$T(p; q_1, q_2) = \int_{4m^2}^{\infty} \frac{ds ds'}{\pi^2} \int d\phi \frac{G_{\text{meson}}(s)}{s - \mu^2} \frac{G_{\text{meson}}(s')}{s' - \mu^2} S_{\text{meson}}.$$

Here s and s' are the invariant masses squared in the intermediate $q\bar{q}$ -states; G_{meson} is the vertex for the $\text{meson} \rightarrow q\bar{q}$ transition. The ratio $G_{\text{meson}}(s)/(s - \mu^2)$ determines the wave function of the produced meson up to the spin factor, and S_{meson} is the spin factor of the loop diagram 2b.

Let us explain the structure of the spectral integral (8) in more detail.

The cut quark loop should be integrated over the phase space of the intermediate $q\bar{q}$ -states, $\Phi(P; k_1, k_2)$ and $\Phi(P'; k'_1, k'_2)$, with the invariant phase space determined as

$$d\Phi(P; k_1, k_2) = \frac{1}{2} \frac{d^3 k_1}{(2\pi)^3 2k_{10}} \frac{d^3 k_2}{(2\pi)^3 2k_{20}} (2\pi)^4 \delta^{(4)}(P - k_1 - k_2). \quad (9)$$

The integration is carried out taking into account the conservation law for momenta which flow through the ladder (wavy lines in Fig. 2b); the momenta are denoted as q_1 and q_2 . Thus, the phase space integration of the cut diagram is given by the expression:

$$d\Phi(P; k_1, k_2) d\Phi(P'; k'_1, k'_2) (2\pi)^3 2k'_{10} \delta^{(3)}(\mathbf{k}'_1 - \mathbf{k}_1 - \mathbf{q}_1) (2\pi)^3 2k'_{20} \delta^{(3)}(\mathbf{k}'_2 - \mathbf{k}_2 + \mathbf{q}_2). \quad (10)$$

Here $k_i^2 = k_j'^2 = m^2$ and $P^2 = s, P'^2 = s'$. We use light cone variables for the wave functions of the produced mesons; the simplest way to introduce them is to use the infinite momentum frame. Then the four-momenta $P = (P_0, \mathbf{P}_\perp, P_z)$ and $k_i = (k_{i0}, \mathbf{k}_{i\perp}, k_{iz})$ are written within the limits $p \rightarrow \infty, k_{iz} \rightarrow \infty, k'_{iz} \rightarrow \infty$. After introducing the light-cone variables ($\xi_i = k_{iz}/p, \xi'_i = k'_{iz}/p, m_{i\perp}^2 = m^2 + k_{i\perp}^2, m_{i\perp}'^2 = m^2 + k_{i\perp}'^2$) and putting q_{iz} small ($q'_{iz}/p \rightarrow 0$, the constraint of the multiperipheral kinematics) we re-write (10) as follows:

$$\begin{aligned} & \frac{1}{16\pi} \cdot \frac{d\xi_1 d\xi_2}{\xi_1 \xi_2} \delta(1 - \xi_1 - \xi_2) d^2 k_{1\perp} d^2 k_{2\perp} \delta^{(2)}(\mathbf{k}_{1\perp} + \mathbf{k}_{2\perp}) \delta \left(s - \frac{m_{1\perp}^2}{\xi_1} - \frac{m_{2\perp}^2}{\xi_2} \right) \\ & \times \delta \left(s' + (\mathbf{q}_{1\perp} - \mathbf{q}_{2\perp})^2 - \frac{m_{1\perp}^2}{\xi_1} - \frac{m_{2\perp}^2}{\xi_2} \right) \cdot (2\pi)^3 2P_0 \delta^{(2)}(\mathbf{P} + \mathbf{q}_1 - \mathbf{q}_2 - \mathbf{P}') \\ & \equiv d\phi(\xi_1, \xi_2; \mathbf{k}_{1\perp}, \mathbf{k}_{2\perp}; \mathbf{q}_{1\perp}, \mathbf{q}_{2\perp}) \cdot (2\pi)^3 2P_0 \delta^{(3)}(\mathbf{P} + \mathbf{q}_1 - \mathbf{q}_2 - \mathbf{P}'). \end{aligned} \quad (11)$$

The factor $d\phi$ stands for the phase space integration in the spectral integral (8): $d\phi \equiv d\phi(\xi_1, \xi_2; \mathbf{k}_{1\perp}, \mathbf{k}_{2\perp}; \mathbf{q}_{1\perp}, \mathbf{q}_{2\perp})$.

In the approximation given by (7), when the jet block inside of the big quark loop is considered as a real process, one may fix $q_1 = q_2 = 0$; then the inclusive cross section is proportional to $T(p; 0, 0)$. Taking δ -functions into account in (11), the formula for $T(p; 0, 0)$ acquires a rather simple form:

$$T(p; 0, 0) = \frac{1}{16\pi^3} \int_0^1 \frac{d\xi}{\xi(1-\xi)} \int d^2 k_\perp \left(\frac{G_{\text{meson}}(s)}{s - \mu^2} \right)^2 S_{\text{meson}} , \quad (12)$$

where $s = m_\perp^2 / (\xi(1-\xi))$.

The amplitude $T(p; 0, 0)$ alone does not determine the inclusive cross section $d\sigma/dx(Z^0 \rightarrow \text{meson} + X)$ because the amplitudes $A(W_1^2, 0)$ and $A(W_2^2, 0)$ depend on ξ and k_\perp^2 , see (5). Taking into account this dependence, one has at $x \sim 0$:

$$\frac{d\sigma}{dx}(Z^0 \rightarrow \text{meson} + X) \sim \frac{1}{16\pi^3} \int_0^1 \frac{d\xi}{\xi(1-\xi)} \int d^2 k_\perp \left(\frac{G_{\text{meson}}(s)}{s - \mu^2} \right)^2 S_{\text{meson}} \Pi(W_1^2, W_2^2) . \quad (13)$$

The spin factor S_{meson} is closely related to the normalization of the wave function of produced meson.

C. Spin factors S_ρ and S_π

Below, we calculate the spin factors S_ρ and S_π at $q_1 = q_2 = 0$. They are:

$$\begin{aligned} S_\pi &= -\text{Sp} \left(i\gamma_5 (\hat{k}_1 + m)(\hat{k}'_1 + m)i\gamma_5 (-\hat{k}'_2 + m)(-\hat{k}_2 + m) \right) \\ S_\rho &= -\text{Sp} \left(\gamma_\alpha^\perp (\hat{k}_1 + m)(\hat{k}'_1 + m)\gamma_\alpha^\perp (-\hat{k}'_2 + m)(-\hat{k}_2 + m) \right) . \end{aligned} \quad (14)$$

We have taken into account here that the quark-gluon ladder carries quantum numbers of the scalar state, $J^P = 0^+$; hence the quark-ladder vertex is unity.

The ρ meson vertex reads:

$$\gamma_\alpha^\perp = g_{\alpha\alpha'}^\perp \gamma_{\alpha'} , \quad g_{\alpha\alpha'}^\perp = g_{\alpha\alpha'} - \frac{P_\alpha P_{\alpha'}}{P^2} . \quad (15)$$

In the spin factor S_ρ the summation is performed over polarizations of the meson. For the spin factors we have:

$$S_\pi = 8m^2 s , \quad S_\rho = 16 m^2 (s + 2m^2) . \quad (16)$$

Let us now demonstrate that similar spin factors determine the normalization of wave functions of the ρ -meson and the pion.

D. Wave functions of the pion and the ρ -meson

In the framework of the light-cone technique it is reasonable to introduce the wave function of a particle and its normalization using the form factor of the particle. The procedure of definition of the wave function is discussed in detail in [29,30]. Schematically, for the $q\bar{q}$ state this procedure looks as follows.

The form factor of a composite system (for definiteness, we consider the pion form factor) is determined by the triangle diagram Fig. 2c, where the photon interacts with the composite system. The form factor is represented as a double spectral integral over masses of the incoming and outgoing pion; corresponding cuttings are shown by the dashed lines I and II in Fig. 2c.

The structure of the amplitude of the triangle diagram for the pion has the following form:

$$A_\nu^{(tr)} = (p_\nu + p'_\nu) F_\pi(q^2) , \quad (17)$$

where p and p' are momenta of the incoming and outgoing pions, the index ν refers to the photon polarization and $F_\pi(q^2)$ is the pion form factor which, in terms of the double spectral representation, can be written as

$$F_\pi(q^2) = \int_{4m^2}^{\infty} \frac{ds ds'}{\pi^2} \int d\phi^{(\text{tr})}(k_1, k'_1, k_2) \frac{G_\pi(s)}{s - \mu^2} T_\pi(s, s', q^2) . \quad (18)$$

Here $d\phi^{(\text{tr})}(k_1, k'_1, k_2)$ is the phase space of the triangle diagram:

$$d\Phi^{(\text{tr})}(k_1, k'_1, k_2) = d\Phi(P; k_1, k_2) d\Phi(P'; k'_1, k'_2) \cdot (2\pi)^3 2k'_{20} \delta^{(3)}(\mathbf{k}'_2 - \mathbf{k}_2) ; \quad (19)$$

P and P' are total momenta of the $q\bar{q}$ system before and after the interaction with the photon: $P = k_1 + k_2$ and $P' = k'_1 + k'_2$, and $P^2 = s$ and $P'^2 = s'$. The spin factor of the triangle diagram, T_π , is determined by the following trace:

$$(-)\text{Sp} \left[i\gamma_5(\hat{k}'_1 + m)\gamma_\nu^\perp(\hat{k}_1 + m)i\gamma_5(-\hat{k}_2 + m) \right] = (P_\nu^\perp + P_\nu'^\perp) T_\pi(s, s', q^2) . \quad (20)$$

The index \perp stands for vectors orthogonal to the photon momentum:

$$\gamma_\nu^\perp = g_{\nu\nu'}^\perp \gamma_{\nu'}, \quad P_\nu^\perp = g_{\nu\nu'}^\perp P_{\nu'}, \quad g_{\nu\nu'}^\perp = g_{\nu\nu'} - \frac{q_\nu q_{\nu'}}{q^2} . \quad (21)$$

At $q^2 = 0$ one has $F_\pi(0) = 1$. Direct calculations of equation (18) in the limit $q^2 \rightarrow 0$ give:

$$1 = \int_{4m^2}^{\infty} \frac{ds}{\pi} \left(\frac{G_\pi(s)}{s - \mu^2} \right)^2 \rho(s) S_\pi^{(wf)}(s) . \quad (22)$$

Here $\rho(s)$ is the phase volume of the $q\bar{q}$ system:

$$\rho(s) = \frac{1}{2} \int d\Phi(P; k_1, k_2) = \frac{1}{16\pi} \sqrt{\frac{s - 4m^2}{s}} , \quad (23)$$

and $S_\pi^{(wf)}(s)$ is the trace of the quark loop diagram for the pion:

$$S_\pi^{(wf)}(s) = (-)\text{Sp} \left[i\gamma_5(\hat{k}_1 + m)i\gamma_5(-\hat{k}_2 + m) \right] = 2s . \quad (24)$$

Using light-cone variables we come to the following form of (22):

$$1 = \frac{1}{16\pi^3} \int_0^1 \frac{d\xi}{\xi(1-\xi)} \int d^2\mathbf{k}_\perp \left(\frac{G_\pi(s)}{s - \mu^2} \right)^2 2s , \quad (25)$$

where $s = (m^2 + k_\perp^2)/(\xi(1-\xi))$. This equation enables us to introduce the pion wave function in the form

$$\psi_\pi(\xi, \mathbf{k}_\perp) = \frac{G_\pi(s)}{s - \mu^2} \sqrt{2s} , \quad (26)$$

which is normalized by the standard requirement.

Likewise, we introduce the ρ -meson wave function: it is defined by the form factor which is the spin matrix $F_{\alpha\alpha'}(q^2)$. In problems that do not deal with polarization properties of the vector particle, it is convenient to work with the trace of the form factor matrix, $\sum_\alpha F_{\alpha\alpha}(q^2)$, which is normalized by

$$\sum_{\alpha=1,2,3} F_{\alpha\alpha}(0) = 3 . \quad (27)$$

The trace $\sum_\alpha F_{\alpha\alpha}(q^2)$ is determined by the expression analogous to (18), with evident substitutions $G_\pi \rightarrow G_\rho$ and $T_\pi \rightarrow T_\rho$. As a result, we obtain the normalization for averaged form factor:

$$1 = \frac{1}{3} \sum_{\alpha=1,2,3} F_{\alpha\alpha}(0) = \int_{4m^2}^{\infty} \frac{ds}{\pi} \left(\frac{g_\rho(s)}{s - \mu^2} \right)^2 \rho(s) S_\rho^{(wf)}(s) , \quad (28)$$

where

$$S_\rho^{(wf)}(s) = -\frac{1}{3} \text{Sp} \left[\left(\gamma_\alpha - P_\alpha \frac{\hat{P}}{P^2} \right) (\hat{k}_1 + m) \left(\gamma_\alpha - P_\alpha \frac{\hat{P}}{P^2} \right) (-\hat{k}_2 + m) \right]. \quad (29)$$

The $\rho \rightarrow q\bar{q}$ vertex, $\gamma_\alpha - P_\alpha \hat{P}/P^2$, selects three degrees of freedom of the ρ -meson. We have :

$$S_\rho^{(wf)}(s) = \frac{4}{3}(s + 2m^2). \quad (30)$$

In the infinite momentum frame, (28) is re-written as:

$$1 = \frac{1}{16\pi^2} \int_0^1 \frac{d\xi}{\xi(1-\xi)} \int d^2\mathbf{k}_\perp \psi_\rho^2(\xi, \mathbf{k}_\perp), \quad (31)$$

where

$$\psi_\rho(\xi, \mathbf{k}_\perp) = \frac{G_\rho(s)}{s - \mu^2} \sqrt{\frac{4}{3}(s + 2m^2)}. \quad (32)$$

E. V/P ratio for the central region and colour degrees of freedom

The normalization conditions for pion and ρ -meson wave functions define unambiguously the ratio of yields for prompt production: $\rho/\pi = 3$, if the wave functions of these mesons are similar. Indeed, the expression (13) represented in terms of wave functions ψ_ρ and ψ_π give us (4) immediately.

We have not taken into account explicitly the colour degrees of freedom in the derivation. This, however, can be easily done. For the $meson \rightarrow q\bar{q}$ vertex the colour operator is equal to $I/\sqrt{N_c}$, where I is a unity matrix in colour space. We have two colour amplitudes, singlet and octet, for the chain of the quark loop diagrams, A_1 and A_8 . The couplings of the amplitudes A_1 and A_8 to quarks ($g(A_1)$ and $g(A_8)$) are proportional to I and λ (Gell-Mann matrices). All colour operators are the same for both pion and ρ -meson production. Because of that, the colour factors are not important for the ratio ρ/π — they are identical and cancel in the production ratio.

As was stated above, the main contribution into inclusive meson production comes from the ladder diagram A_8 . This is due to the fact that the coupling constant for the amplitude with $c = 8$ is larger than for $c = 1$. In terms of $1/N_c$ expansion $g(A_1)/g(A_8) \sim 1/\sqrt{N_c}$.

III. INCLUSIVE PRODUCTION OF MESONS IN THE FRAGMENTATION REGION

The inclusive production cross section of mesons in the fragmentation region is determined by the discontinuity of the diagram 2d. The spectral representation for this diagram is written as an integral over the masses of initial and final $q\bar{q}$ states in the transitions $Z^0 \rightarrow q\bar{q}$ and $q\bar{q} \rightarrow Z^0$ and over $q\bar{q}$ masses in the transitions $q\bar{q} \rightarrow meson$ and $meson \rightarrow q\bar{q}$. The amplitude of the diagram of Fig. 2d reads:

$$\begin{aligned} & \int_{4m^2}^{\infty} \frac{dM^2 dM'^2}{\pi^2} \frac{g_Z(M^2) g_Z(M'^2)}{(M^2 - M_Z^2)(M'^2 - M_Z^2)} \int_{4m^2}^{\infty} \frac{ds ds'}{\pi^2} \psi_{meson}(s) \psi_{meson}(s') \\ & \times d\phi_3(k_1, k_2, k_3) d\phi_3(k'_1, k'_2, k'_3) A(W^2, (k_2 - k'_2)^2) \frac{S_{meson}^{(fr)}}{\sqrt{S_{meson}^{(wf)}(s) S_{meson}^{(wf)}(s')}}. \end{aligned} \quad (33)$$

The vertices $g_Z(M^2)$ and $g_Z(M'^2)$ are written for the $Z^0 \rightarrow q\bar{q}$ and $q\bar{q} \rightarrow Z^0$ transitions. Spectral integrals over s and s' stand for $q\bar{q} \rightarrow meson$ and $meson \rightarrow q\bar{q}$ (where $meson$ means π, ρ). The wave function ψ_{meson} of the produced meson was introduced in an explicit form in Section 2 for the pion and the ρ -meson, and the factors $d\phi_3(k_1, k_2, k_3)$ and $d\phi_3(k'_1, k'_2, k'_3)$ define the integration over phase spaces in the left- and right-hand parts of the diagram of Fig. 2d:

$$d\phi_3(k_1, k_2, k_3) = \frac{1}{2} \frac{d^3 k_1}{(2\pi)^3 2k_{10}} \frac{d^3 k_2}{(2\pi)^3 2k_{20}} ,$$

$$\times (2\pi)^4 \delta^{(4)}(\tilde{P} - k_1 - k_2) \frac{1}{2} \frac{d^3 k_3}{(2\pi)^3 2k_{30}} (2\pi)^4 \delta^{(4)}(P - k_1 - k_3) . \quad (34)$$

Here $\tilde{P}^2 = M^2$ and $P^2 = s$.

The block $A(W^2, (k_2 - k'_2))$ defines the multiperipheral ladder (wavy line in Fig. 2d). This block depends on the momentum transfer squared $(k_2 - k'_2)^2$ and the total energy squared W^2 :

$$W^2 \simeq M_Z^2(1 - x) ; \quad (35)$$

x is the momentum fraction carried by the produced meson: $x = 2p/M_z$, where p is the longitudinal component of meson momentum, $p_{\text{meson}} = (p + \mu_1^2/2p, 0, p)$.

The spectra $d\sigma(Z^0 \rightarrow \text{meson} + X)/dx$ fall rapidly with increasing x : this decrease is governed by $A(W^2, (k_2 - k'_2))$.

All the characteristics of (33) listed above are the same for both pion and ρ -meson production, the wave functions ψ_π and ψ_ρ are also supposed to be the same. The difference may be contained in the spin factors $S_\pi^{(fr)}$ and $S_\rho^{(fr)}$ which are

$$S_\pi^{(fr)} = (-)\text{Sp} \left[\gamma_\nu^\perp (1 + R\gamma_5)(\hat{k}'_1 + m)i\gamma_5(\hat{k}'_3 + m)(\hat{k}_3 + m) \right. \\ \left. \times i\gamma_5(\hat{k}_1 + m)\gamma_\nu^\perp (1 + R\gamma_5)(-\hat{k}_2 + m)(-\hat{k}'_2 + m) \right];$$

$$S_\rho^{(fr)} = (-)\text{Sp} \left[\gamma_\nu^\perp (1 + R\gamma_5)(\hat{k}'_1 + m)\gamma_\alpha^\perp(\hat{k}'_3 + m)(\hat{k}_3 + m) \right. \\ \left. \times \gamma_\alpha^\perp(\hat{k}_1 + m)\gamma_\nu^\perp (1 + R\gamma_5)(-\hat{k}_2 + m)(-\hat{k}'_2 + m) \right]. \quad (36)$$

The factor $\gamma_\nu^\perp(1 + R\gamma_5)$ is related to the vertex $Z^0 \rightarrow q\bar{q}$ which is determined by the vector and axial-vector interactions (the ratio of coupling constants is ~ 2.63 for the u quark and ~ 1.43 for the d quark). For $S_\pi^{(fr)}$ the summation is performed over polarizations of the Z^0 boson (index ν); γ_ν^\perp is orthogonal to $k_1 + k_2$ and $\gamma_\nu'^\perp$ is orthogonal to $k'_1 + k'_2$. For the ρ -meson spin factor $S_\rho^{(fr)}$, the summation is performed over polarizations of the Z^0 boson (index ν) and ρ -meson (index α) with $\gamma_\alpha^\perp \perp (k_1 + k_3)$ and $\gamma_\alpha'^\perp \perp (k'_1 + k'_3)$ (see also (15)).

Normalization factors $S_{\text{meson}}^{(wf)}(s)$ and $S_{\text{meson}}^{(wf)}(s')$ in (33) are related to the definition of meson wave functions, see (26) and (32). The explicit expressions for spin factors (36) are presented in Appendix B. Using these expressions, we have an opportunity to perform numerical evaluation of ratios of prompt meson yields in the decay reactions with smaller energy release. In the case of the Z^0 decay, when $M_Z \gg m$ and $M_Z \gg \mu$, a reasonably good approximation for (33) is to substitute the integrals over M^2 and M'^2 by semi-residues in the poles $M^2 = M_z^2$ and $M'^2 = M_z'^2$. Then we have the following kinematics for real jets:

$$k_1 = k'_1 , \quad k_2 = k'_2 . \quad (37)$$

In this approximation we can put $k_3 = k'_3$ and $s = s'$. Then we have for light mesons:

$$\frac{S_\pi^{(fr)}}{S_\pi^{(wf)}} \simeq 2M_Z^2(1 + R^2) , \quad \frac{S_\rho^{(fr)}}{S_\rho^{(wf)}} \simeq 6M_Z^2(1 + R^2) , \quad (38)$$

which gives the ratio of the prompt yields $\rho : \pi = 3 : 1$ in the fragmentation region $x \sim 0.5 - 1$ (more generally, $V : P = 3 : 1$ for hadronic decays $Z^0 \rightarrow q\bar{q}$ with $q = u, d, s$).

The same ratio appears for the production of heavy quarks $Z^0 = Q\bar{Q}$, where $Q = c, b$. For example, in the case of b quark the spin factors are:

$$\frac{S_B^{(fr)}}{S_B^{(wf)}} \simeq 2 [M_Z^2 + 2m_b^2 + R^2(M_Z^2 - 4m_b^2)] ,$$

$$\frac{S_{B^*}^{(fr)}}{S_{B^*}^{(wf)}} = 6 [M_Z^2 + 2m_b^2 + R^2(M_Z^2 - 4m_b^2)] , \quad (39)$$

and thus the ratio $B_{\text{prompt}}^* : B_{\text{prompt}}$ also equals 3.

A. V/P ratio in the fragmentation region: comparison to data

We have seen that $V/P = 3$ in the fragmentation region as well as in the central region. However, in the central region the comparison of quark combinatorics with experiment is hampered by the presence of a number of the decay products of highly excited resonances, while in the fragmentation region this contribution is suppressed by rapidly decreasing spectra. This means that the fragmentation region allows us to perform a model-independent verification of quark combinatorics. Here we carry out such a comparison based on the ALEPH data [11].

To operate with meson spectra at $x \sim 0.2 - 0.8$ we have fitted the spectra $(1/\sigma_{tot})d\sigma/dx$ to the sum of exponents $\sum C_i e^{-b_i x}$; the calculation results are presented in Fig. 3 for π^\pm, π^0, ρ^0 and (p, \bar{p}) . The ratio of fitting curves drawn with calculation errors (shaded area) is shown in Fig. 4a for ρ/π . We see that for $0.6 < x < 0.8$ the data are in reasonable agreement with the prediction $\rho/\pi = 3$.

The figure 4b,c demonstrates the ratios K^{*0}/K^0 and $K^{*\pm}/K^\pm$: the data do not contradict the prediction, though the errors are too large to conclude anything more definite.

IV. SUPPRESSION OF THE STRANGE AND HEAVY QUARK PRODUCTIONS

In hadronic multiparticle production processes (in jet processes of the type of $Z^0 \rightarrow \text{hadrons}$ or in hadron-hadron collisions at high energies) the production of strange quarks is suppressed. Strong suppression is observed for the production of heavy quarks $Q = c, b$. One can guess that this suppression, being of the same nature for different reactions, is related to the mechanism of the production of new quarks at large separations of colour objects. This mechanism is seen in its pure form in the two-particle decays (the corresponding diagram is shown in Fig. 5a). The block of the production of a new $q\bar{q}$ pair in the two-particle decay is the same as that of meson production in jet processes (Fig. 5b), so it is reasonable to suppose that the suppression mechanism of the production of new quarks is similar for these processes.

A. Two-meson decay of the $q\bar{q}$ state and soft hadronization

The decay of the $q\bar{q}$ state takes place as follows: the quarks of the excited state leave the region where they were kept by the confinement barrier, and at a sufficiently large separation a new quark-antiquark pair will be produced inevitably: together with the incident quarks, these new quarks then form mesons (i.e. free particles). Schematically, this process (which is the leading one in terms of the $1/N$ expansion) is shown on the diagram of Fig. 5a: two quarks fly away (with the momenta p_1 and p_2), and at large quark separations the gluonic field produces a new $q\bar{q}$ pair (the quarks with momenta k_2, k_3); then the primary quark (now with momentum k_1) joins the newly-born one (k_2) creating a meson. Likewise, another newly-born quark (k_3) joins the other primary quark (now with momentum k_4) producing the second meson.

The block with the quark-antiquark production, that is the transition

$$q(p_1) + \bar{q}(p_2) \rightarrow q(k_1) + \bar{q}(k_2) + q(k_3) + \bar{q}(k_4) \quad (40)$$

is the key process that determines the decay physics; it is shown separately in Fig. 5c. The process (40) is responsible for the leaving the confinement trap by quarks. In modelling the hadronization transition amplitude (40), quark combinatorics uses the hypothesis of soft hadronization. The idea was formulated at the 70's, and even now the soft hadronization hypothesis looks rather reliable and productive. It suggests that in the ladder of produced quarks (Figs. 1a, 5c) the contribution comes from small momentum transfers (of the order of $R_{confinement}^{-2}$). In the framework of the space-time picture this means that new $q\bar{q}$ pairs are produced at large separations, when colour objects leave the confinement well.

The soft hadronization hypothesis applied to the decay processes treats the ladder diagram of Fig. 5c for the decay amplitude of Fig. 5a in the same way as for jet production, Fig. 5b: process (40) is an elementary subprocess both for the high-energy ladder and the two-particle decay amplitude, and the momentum transfers which enter the amplitude (40) appear to be small in the hadronic scale, $\sim R_{confinement}^{-2}$.

B. Spectral representation of the decay diagram

Below we consider in detail the decay amplitude of Fig. 5a, performing calculations, as is done before, in the framework of the spectral representation with the light-cone wave functions for $q\bar{q}$ states.

By using the notations

$$\begin{aligned} P &= p_1 + p_2, \quad k_{12} = k_1 + k_2, \quad k_{34} = k_3 + k_4, \\ M^2 &= (k_1 + k_2)^2, \quad s_{12} = (k_1 + k_2)^2, \quad s_{34} = (k_3 + k_4)^2 \end{aligned} \quad (41)$$

we have the following spectral representation for the amplitude of the diagram shown in Fig. 5a:

$$\begin{aligned} A(q\bar{q} \text{ state} \rightarrow \text{two mesons}) &= \int_{4m^2}^{\infty} \frac{dM^2}{\pi} \Psi_{in}(M^2) d\Phi(P; p_1, p_2) \int_{(m+m_s)}^{\infty} \frac{ds_{12} ds_{34}}{\pi^2} \\ &\times t(p_1, p_2; k_1, k_2, k_3, k_4) d\Phi(k_{12}; k_1, k_2) d\Phi(k_{34}; k_3, k_4) \Psi_1(s_{12}) \Psi_2(s_{34}). \end{aligned} \quad (42)$$

Here the masses of newly-born quarks $i = 2, 3$ are denoted as m_s , thus opening the way to consider the decay with strange quark production. The transition amplitude (40) of Fig. 5c is denoted as $t(p_1, p_2; k_1, k_2, k_3, k_4)$. The decay amplitude (42) is written in terms of meson wave functions: for the initial state it is $\Psi_{in}(M^2)$, and for outgoing mesons they are $\Psi_1(s_{12})$ and $\Psi_2(s_{34})$. We do not specify here the meson spin structure of the quark propagator: we consider it below in a more detailed consideration of the transition amplitude (40).

Thus, the decay amplitude A is a convolution of the transition amplitude (40) with wave functions of initial and outgoing mesons:

$$A(q\bar{q} \text{ state} \rightarrow \text{two mesons}) = \Psi_{in} \otimes t \otimes \Psi_1 \Psi_2. \quad (43)$$

Further, we use light-cone variables; with $p_{iz} \rightarrow \infty$ and $k_{iz} \rightarrow \infty$ we have

$$\begin{aligned} k_i &= (k_{iz} + \frac{m^2 + k_{i\perp}^2}{2k_{iz}}, \mathbf{k}_{i\perp}, k_{iz}) \quad i = 1, 4 \\ k_i &= (k_{iz} + \frac{m_s^2 + k_{i\perp}^2}{2k_{iz}}, \mathbf{k}_{i\perp}, k_{iz}) \quad i = 2, 3 \\ p_1 &= (p_{iz} + \frac{m^2 + p_{i\perp}^2}{2p_{iz}}, \mathbf{p}_{i\perp}, p_{iz}), \quad i = 1, 2. \end{aligned} \quad (44)$$

Let us use the frame where the outgoing particles are moving along the z -axis. We put

$$\begin{aligned} P &= (P_z + \frac{M^2}{2P_z}, 0, P_z), \\ k_{12} &= (k_{12z} + \frac{s_{12}}{2k_{12z}}, 0, k_{12z}), \\ k_{34} &= (k_{34z} + \frac{s_{34}}{2k_{34z}}, 0, k_{34z}). \end{aligned} \quad (45)$$

The phase spaces $d\Phi(k_{12}; k_1, k_2)$, $d\Phi(k_{34}; k_3, k_4)$ contain the energy-momentum conservation δ -functions which give

$$\begin{aligned} M^2 &= \frac{m^2 + p_{1\perp}^2}{x_1} + \frac{m^2 + p_{2\perp}^2}{x_2}, \\ s_{12} &= \frac{m^2 + k_{1\perp}^2}{y_1} + \frac{m_s^2 + k_{2\perp}^2}{y_2}, \\ s_{34} &= \frac{m_s^2 + k_{3\perp}^2}{y_3} + \frac{m^2 + k_{4\perp}^2}{y_4}. \end{aligned} \quad (46)$$

Here $x_i = p_{iz}/(p_{1z} + p_{2z})$, $y_i = k_{iz}/(k_{1z} + k_{2z})$ for $i = 1, 2$ and $y_i = k_{iz}/(k_{3z} + k_{4z})$ for $i = 3, 4$.

C. The region of dominance of the transition amplitude $t_{q\bar{q} \rightarrow q\bar{q}q\bar{q}}$

Let us turn to the principal point, namely: the evaluation of the region in momentum space selected by the transition amplitude of Fig. 5c within the soft hadronization assumption.

The hypothesis of soft hadronization means that the ladder diagram of Fig. 5c has a peripheral structure: it requires the momentum transfers squared to the $q\bar{q}$ block to be small, of the order of $1/R_{\text{confinement}}^2$. So

$$\begin{aligned}
-(p_1 - k_1)^2 &\simeq (\mathbf{p}_{1\perp} - \mathbf{k}_{1\perp})^2 \sim R_{\text{confinement}}^{-2} , \\
-(p_2 - k_4)^2 &\simeq (\mathbf{p}_{2\perp} - \mathbf{k}_{4\perp})^2 \sim R_{\text{confinement}}^{-2} .
\end{aligned} \tag{47}$$

Likewise, the momentum transfer squared in the quark propagator (see Fig. 5c) is of the order:

$$(p_1 - k_1 - k_2)^2 \simeq -(\mathbf{p}_{1\perp} - \mathbf{k}_{1\perp} - \mathbf{k}_{2\perp})^2. \tag{48}$$

Let us now discuss the peripheral constraint (47) in more detail. As an example, let us consider $(p_1 - k_1)^2$. We have

$$\begin{aligned}
(p_1 - k_1)^2 &= (p_{1z} - k_{1z} + \frac{m^2 + p_{1\perp}^2}{2p_{1z}} - \frac{m^2 + k_{1\perp}^2}{2k_{1z}})^2 , \\
&\quad -(\mathbf{p}_{1\perp} - \mathbf{k}_{1\perp})^2 - (p_{1z} - k_{1z})^2 .
\end{aligned} \tag{49}$$

The gluon carries a small fraction of the longitudinal momentum of the primary quark, therefore

$$p_{1z} \gg p_{1z} - k_{1z} \equiv \Delta. \tag{50}$$

Then

$$(k_1 - p_1)^2 \simeq \frac{\Delta}{p_{1z}} (k_{1\perp}^2 - p_{1\perp}^2) - (\mathbf{k}_{1\perp} - \mathbf{p}_{1\perp})^2 \simeq -(\mathbf{k}_{\perp} - \mathbf{p}_{1\perp})^2. \tag{51}$$

The peripheral constraint means that $y_1 \gg y_2$. But in numerical calculations this does not require very large invariant energies squared, s_{12} and s_{34} , which determine the blocks of quark fusion. For example, at $y_2/y_1 \sim 1/10$ one has $s_{12} \sim 10m^2 \sim 1 \text{ GeV}^2$ for $m \simeq 350 \text{ MeV}$, which gives for the quark relative momentum the value of the order of $300 - 400 \text{ MeV}$.

D. The decay amplitude $A(q\bar{q} \text{ state} \rightarrow \text{two mesons})$

Let us now write the formula for $t(p_1, p_2; k_1, k_2, k_3, k_4)$ in the simplest approximation, taking into account the t -channel propagators only:

$$\begin{aligned}
t(p_1, p_2; k_1, k_2, k_3, k_4) &= \frac{g}{m_g^2 + (\mathbf{p}_{1\perp} - \mathbf{k}_{1\perp})^2} \\
&\times \frac{g^2 (m_s - \gamma(\mathbf{p}_{1\perp} - \mathbf{k}_{1\perp} - \mathbf{k}_{2\perp}))}{m_s^2 + (\mathbf{p}_{1\perp} - \mathbf{k}_{1\perp} - \mathbf{k}_{2\perp})^2} \cdot \frac{g}{m_g^2 + (\mathbf{p}_{2\perp} - \mathbf{k}_{4\perp})^2}
\end{aligned} \tag{52}$$

To avoid ultrared divergence, the effective mass of the soft gluon is introduced into the gluon propagator (see, for example, [31]).

The equation (52) does not state that the transition amplitude $t(p_1, p_2; k_1, k_2, k_3, k_4)$ selects large distances. At this point the amplitude (52) may be improved by incorporating form factors into the gluon emission vertex:

$$g \rightarrow g((\mathbf{p}_{1\perp} - \mathbf{k}_{1\perp})^2), \quad g \rightarrow g((\mathbf{p}_{2\perp} - \mathbf{k}_{4\perp})^2). \tag{53}$$

With equations (52) and (53) the amplitude A reads:

$$\begin{aligned}
A(q\bar{q} \text{ state} \rightarrow \text{two mesons}) &= \int_0^1 \frac{dx_1 dx_2 \delta(1 - x_1 - x_2)}{16\pi^2 x_1 x_2} d\mathbf{p}_{1\perp} d\mathbf{p}_{2\perp} \delta(\mathbf{p}_{1\perp} + \mathbf{p}_{1\perp}) \\
&\times \int_{y_1 \gg y_2} \frac{dy_1 dy_2 \delta(1 - y_1 - y_2)}{16\pi^2 y_1 y_2} \cdot d\mathbf{k}_{1\perp} d\mathbf{k}_{2\perp} \delta(\mathbf{k}_{1\perp} + \mathbf{k}_{2\perp}) \\
&\times \int_{y_4 \gg y_3} \frac{dy_3 dy_4 \delta(1 - y_3 - y_4)}{16\pi^2 y_3 y_4} d\mathbf{k}_{3\perp} d\mathbf{k}_{4\perp} \delta(\mathbf{k}_{3\perp} + \mathbf{k}_{4\perp}) \Psi_{in}(x_1, x_2; \mathbf{p}_{1\perp}, \mathbf{p}_{2\perp}) \\
&\times \frac{g((\mathbf{p}_{1\perp} - \mathbf{k}_{1\perp})^2)}{m_g^2 + (\mathbf{p}_{1\perp} - \mathbf{k}_{1\perp})^2} \frac{g^2 (m_s - \gamma(\mathbf{p}_{1\perp} - \mathbf{k}_{1\perp} - \mathbf{k}_{2\perp}))}{m_s^2 + (\mathbf{p}_{1\perp} - \mathbf{k}_{1\perp} - \mathbf{k}_{2\perp})^2} \frac{g((\mathbf{p}_{2\perp} - \mathbf{k}_{4\perp})^2)}{m_g^2 + (\mathbf{p}_{2\perp} - \mathbf{k}_{4\perp})^2} \\
&\times \Psi_1(y_1, y_2; \mathbf{k}_{1\perp}, \mathbf{k}_{2\perp}) \Psi_2(y_3, y_4; \mathbf{k}_{3\perp}, \mathbf{k}_{4\perp}).
\end{aligned} \tag{54}$$

This is the expression for the decay amplitude which makes it possible to discuss the rules of quark combinatorics.

In a rough approximation that still gives a qualitatively correct answer, we neglect the momenta in the propagator of newly-born quarks:

$$\frac{g^2 (m_s - \gamma(\mathbf{p}_{1\perp} - \mathbf{k}_{1\perp} - \mathbf{k}_{2\perp}))}{m_s^2 + (\mathbf{p}_{1\perp} - \mathbf{k}_{1\perp} - \mathbf{k}_{2\perp})^2} \rightarrow \frac{g^2}{m_s} . \quad (55)$$

We have

$$A(q\bar{q} \text{ state} \rightarrow \text{two mesons}) = \frac{\alpha_s}{m_s} \cdot (\Psi_{in} \otimes t \otimes \Psi_1 \Psi_2) , \quad (56)$$

This equation tells us that the probability to produce non-strange and strange quarks, $u\bar{u} : d\bar{d} : s\bar{s} = 1 : 1 : \lambda$, is determined by the ratio of masses squared of non-strange (u, d) to strange (s) quark. Introducing the constituent quark masses in the soft region, $m_u \simeq m_d \equiv m = 350$ MeV and $m_s \simeq 500$ MeV, we get:

$$\lambda \simeq \frac{m^2}{m_s^2} \simeq 0.5 . \quad (57)$$

The equations (55) and (56) justify the statements of quark combinatorics applied to the decay processes [7–9,32]. Of course, we here suppose the identity of meson wave functions belonging to the same multiplet.

The equation (57) gives us a rough evaluation of λ , for in (55) we neglected momentum transfers squared that are compatible with light quark masses. In more sophisticated evaluations of λ , one may take into account the momentum dependence of the quark propagator:

$$\frac{1}{m_s^2 + (\mathbf{p}_{1\perp} - \mathbf{k}_{1\perp} - \mathbf{k}_{2\perp})^2} \rightarrow \frac{1}{m_s^2 + \langle k^2 \rangle} , \quad (58)$$

where $\langle k^2 \rangle$ is a typical momentum squared inherent to the considered decay process. Therefore,

$$\lambda = \frac{m^2 + \langle k^2 \rangle}{m_s^2 + \langle k^2 \rangle} . \quad (59)$$

For standard decays of light resonances $\langle k^2 \rangle \sim 0.1 - 0.3$ (GeV/c)², and this results in the increase of λ compared to the estimation (57). Indeed, in the analysis [32] $\lambda \sim 0.7$ was found. Actually, equation (59) demonstrates that λ can vary depending on different types of reactions.

E. Suppression parameter λ in the hadronic Z^0 decay

Now let us turn to the processes of the $q\bar{q}$ pair production in jet processes $Z^0 \rightarrow q\bar{q} \rightarrow \text{hadrons}$, which is shown in Fig. 5b. All the above considerations, which have been used for the decay of a resonance into two mesons, may be applied to this process. As a result, we obtain the following formula which is a counterpart of (56):

$$A(Z^0 \rightarrow \text{two mesons} + X) = \frac{\alpha_s}{m_s} \cdot (q\bar{q} \text{ from jet ladder} \otimes t \otimes \Psi_1 \Psi_2) . \quad (60)$$

This formula differs from (56) by the initial state only, which is the wave function of $q\bar{q}$ -pair for jet ladder but not for the state defined by the wave function Ψ_{in} . This means that the ratio of probabilities of producing a strange and a non-strange quark are given by the factor m^2/m_s^2 . So, like in the decay process, one has:

$$\lambda \simeq \frac{m^2}{m_s^2} \simeq 0.5 . \quad (61)$$

Experimental data on the ratio of yields K^\pm/π^\pm do not contradict this evaluation. The ratio K^\pm/π^\pm as a function of x is shown in Fig. 4e. It is seen that at $x = 0.2$ $K^\pm/\pi^\pm \simeq 0.35$. With the increase of x the ratio K^\pm/π^\pm grows and reaches the value ~ 0.8 at $x = 0.7$. Such an increase is rather legible: the matter is that K mesons are produced both due to the formation of a new $s\bar{s}$ pair in the ladder (with the probability λ) and fragmentation production of $s\bar{s}$ pair in the transition $Z^0 \rightarrow s\bar{s}$. Relative probabilities of prompt production of $Z^0 \rightarrow u\bar{u}, d\bar{d}, s\bar{s}$ obey the ratio $u\bar{u} : d\bar{d} : s\bar{s} \simeq 0.26 : 0.37 : 0.37$. Because of that the production of K meson at large x is proportional to

$$K^+ \sim (0.37 \cdot 1 + 0.26 \cdot \lambda) . \quad (62)$$

Let us comment this formula in a more detail. The K^+ meson is produced in the two processes: (i) fragmentation production of \bar{s} quark (relative probability 0.37) and subsequent pick-up of the u quark from $q\bar{q}$ sea in a jet (relative probability 1), and (ii) fragmentation production of u quark (relative probability 0.26) and pick-up of \bar{s} quark from the sea (relative probability λ).

The same quantity for pions is

$$\pi^+ \sim (0.37 \cdot 1 + 0.26 \cdot 1) . \quad (63)$$

So, the ratio K^+/π^+ at large x is equal to

$$\frac{K^+}{\pi^+} = \frac{0.37 + 0.26\lambda}{0.37 + 0.26} \simeq 0.8 \quad (64)$$

at $\lambda = 0.5$. This value agrees with the experimental data [22] as it is demonstrated by Fig. 4e, where $\lambda(x)$ determined as the $K^\pm/\pi^\pm(x)$ -ratio is shown.

The small value of K^+/π^+ at $x = 0$ is a direct consequence of large probability to produce highly excited resonances: in the resonance decay more pions than kaons are produced. For the problem of breeding of strange and non-strange states in the decay, it is rather interesting to see the ratio K^*/ρ — experimental data for K^{0*}/ρ^0 are shown in Fig. 4e too (shaded area). Remarkably, the ratio K^{0*}/ρ^0 has no tendency to decrease with decreasing x : this means that the rate of breeding of K^{0*} and ρ^0 in decays is approximately the same. Unfortunately, experimental errors are too large to have more definite conclusions about the behaviour of $\lambda(x)$.

F. Production of heavy quarks

The suppression parameter for the production of a strange quark cannot be reliably determined. This is because the masses of strange and non-strange quarks are small compared to the mean transverse momenta of quarks in the production process, see (59). We can draw a more definite conclusion about the suppression parameter λ_Q for the production of heavy quarks $Q = c, b$. This parameter is defined by the same formula (54) for multiperipheral production, so we have:

$$\lambda_Q \simeq \frac{m^2}{m_Q^2 \ln^2 \frac{\Lambda^2}{m_Q^2}} . \quad (65)$$

Here we take into account that the gluon-quark coupling constant decreases with the growth of the quark mass, $\lambda_Q \sim \alpha^2(m_Q^2)$. The QCD scale constant, Λ , is of the order of 200 MeV.

To estimate λ_c and λ_b , let us use $m = 0.35$ GeV, $m_c = M_{J/\Psi}/2 = 1.55$ GeV, $m_b = M_\Upsilon/2 = 4.73$ GeV and $\Lambda = 0.2$ GeV. Then

$$\lambda_c \simeq 2.8 \cdot 10^{-3}, \quad \lambda_b \simeq 1.1 \cdot 10^{-4} . \quad (66)$$

The value of λ_c should reveal itself in the inclusive production of J/Ψ and χ mesons, while λ_b is to be seen in reactions with Υ 's: $Z^0 \rightarrow (\sum J/\Psi + \sum \chi) + X$ and $Z^0 \rightarrow \sum \Upsilon + X$. These reactions are determined by the processes $Z^0 \rightarrow c\bar{c} \rightarrow c + (\bar{c}c + \bar{q}q\text{-sea}) + \bar{c}$ and $Z^0 \rightarrow b\bar{b} \rightarrow b + (\bar{b}b + \bar{q}q\text{-sea}) + \bar{b}$: for the production of a $c\bar{c}$ or $b\bar{b}$ meson a new pair of heavy quarks should be produced, since the quarks formed at the first stage of the decay, $Z^0 \rightarrow c\bar{c}$ or $Z^0 \rightarrow b\bar{b}$, have a rather big gap in the rapidity scale. So, within the definition

$$\begin{aligned} \lambda_c &\simeq \Gamma\left(c\bar{c} \rightarrow c + (\bar{c}c + \bar{q}q\text{-sea}) + \bar{c}\right) / \Gamma(c\bar{c}) \\ \lambda_b &\simeq \Gamma\left(b\bar{b} \rightarrow b + (\bar{b}b + \bar{q}q\text{-sea}) + \bar{b}\right) / \Gamma(b\bar{b}), \end{aligned} \quad (67)$$

we estimate $\Gamma(c\bar{c} \rightarrow c + (\bar{c}c + \bar{q}q\text{-sea}) + \bar{c})$ and $\Gamma(b\bar{b} \rightarrow b + (\bar{b}b + \bar{q}q\text{-sea}) + \bar{b})$ by the available data from [10]:

$$\begin{aligned} \Gamma\left(c\bar{c} \rightarrow c + (\bar{c}c + \bar{q}q\text{-sea}) + \bar{c}\right) &\sim \Gamma\left(J/\Psi(1S)X\right) + \Gamma\left(J/\Psi(2S)X\right) + \Gamma\left(\chi(1P)X\right), \\ \Gamma\left(b\bar{b} \rightarrow b + (\bar{b}b + \bar{q}q\text{-sea}) + \bar{b}\right) &\sim \Gamma\left(\Upsilon(1S)X\right) + \Gamma\left(\Upsilon(2S)X\right) + \Gamma\left(\Upsilon(3S)X\right). \end{aligned} \quad (68)$$

Experiment gives [10]:

$$\begin{aligned}
\Gamma(c\bar{c})/\Gamma(hadrons) &= 0.177 \pm 0.008, \\
\Gamma(b\bar{b})/\Gamma(hadrons) &= 0.217 \pm 0.001, \\
\Gamma\left(J/\Psi(1S)X + J/\Psi(2S)X + \chi(1P)X\right)/\Gamma(hadrons) &= (1.17 \pm 0.13) \cdot 10^{-2}, \\
\Gamma\left(\Upsilon(1S)X + \Upsilon(2S)X + \Upsilon(3S)X\right)/\Gamma(hadrons) &= (1.4 \pm 0.9) \cdot 10^{-4}.
\end{aligned} \tag{69}$$

Thus, we have

$$\begin{aligned}
\Gamma\left(J/\Psi(1S)X + J/\Psi(2S)X + \chi(1P)X\right)/\Gamma(c\bar{c}) &= (2.07 \pm 0.23) \cdot 10^{-3}, \\
\Gamma\left(\Upsilon(1S)X + \Upsilon(2S)X + \Upsilon(3S)X\right)/\Gamma(b\bar{b}) &= (0.31 \pm 0.19) \cdot 10^{-4},
\end{aligned} \tag{70}$$

in a reasonable agreement with (66).

V. THE PROBLEM OF SATURATION OF THE PRODUCED $Q\bar{Q}$ AND QQQ STATES BY MESONS AND BARYONS; BARYON-MESON RATIO AND THE WATSON-MIGDAL FACTOR

In quark combinatorics formulated in [1,2] the baryon quark number reveals itself as the probability to produce a baryon containing this quark. For the hadronization of the quark q_i in (q, \bar{q}) -sea the production rule reads:

$$q_i + (q, \bar{q})_{\text{sea}} \rightarrow \frac{1}{3}B_i + \frac{2}{3}M_i + \frac{1}{3}M + (M, B, \bar{B})_{\text{sea}}, \tag{71}$$

where B_i and M_i are baryons and mesons containing the quark q_i and M , B and \bar{B} are mesons, baryons and antibaryons of the sea.

Generally one can write

$$M = \sum_L \mu_L M_L, \quad B = \sum_L \beta_L M_L, \tag{72}$$

$$M_i = \sum_L \mu_L^{(i)} M_L^{(i)}, \quad B_i = \sum_L \beta_L^{(i)} M_L^{(i)}.$$

where indices $L = 0, 1, 2, \dots$ define the multiplet, while μ_L , $\mu_L^{(i)}$ and β_L , $\beta_L^{(i)}$ are production probabilities of mesons and baryons of the given multiplet in the process of quark hadronization. These probabilities are determined by characteristic relative momenta of the fused quarks.

A. The baryon-meson ratio

Our present understanding of the multiperipheral ladder is not sufficient to re-analyse (71) on the level carried out in Sections 2 and 3 for V/P . Nevertheless, the data for decays $Z^0 \rightarrow p + X$ and $Z^0 \rightarrow \pi^+ + X$ definitely confirm the equation (71). Quark combinatorics [5] predict for p/π^+ at large x :

$$p/\pi^+ \simeq 0.20 \tag{73}$$

In Fig. 4d one can see the p/π^+ ratio given by the fit to the data [11] (shaded area) and the prediction of quark combinatorics (73): the agreement at $x > 0.2$ is quite good.

Let us comment the result of our calculation $p/\pi^+ \simeq 0.20$ for leading particles in jets. In the jet created by a quark the leading hadrons are produced in proportions as it is given by eq. (71): $B_i : 2M_i : M$. We consider only the production of hadrons belonging to the lowest (baryon and meson) multiplets, and, hence, keep in (72) only the

terms with $L = 0$ (hadrons from the quark S -wave multiplets). In our estimations we assume $\beta_0 \simeq \mu_0$, and therefore we substitute $B_i \rightarrow B_i(0)$, $M_i \rightarrow M_i(0)$ and $M \rightarrow M(0)$. The precise content of $B_i(0)$, $M_i(0)$ and $M(0)$ depends on the proportions in which the sea quarks are produced. We assume flavour symmetry breaking for sea quarks, $u\bar{u}:d\bar{d}:s\bar{s} = 1:1:\lambda$, with $0 \leq \lambda \leq 1$. For the sake of simplicity, we put first $\lambda = 0$ (actually the ratio p/π depends weakly on λ). Then for the u -quark initiated jet we have:

$$\begin{aligned} B_u(0) &\rightarrow \frac{2}{15}p + \frac{1}{15}n + (\Delta - \text{resonances}), \\ M_u(0) &\rightarrow \frac{1}{8}\pi^+ + \frac{1}{16}\pi^0 + \frac{1}{16}(\eta + \eta') + (\text{vector mesons}), \\ M(0) &\rightarrow \frac{1}{16}\pi^+ + \frac{1}{16}\pi^0 + \frac{1}{16}\pi^- + \frac{1}{16}(\eta + \eta') + (\text{vector mesons}). \end{aligned} \quad (74)$$

The hadron content of the d -quark initiated jet is determined by isotopic conjugation $p \rightarrow n$, $n \rightarrow p$, $\pi^+ \rightarrow \pi^-$, and the content of antiquark jets is governed by charge conjugation; in jets of strange quarks only sea mesons (M) contribute to the p/π^+ ratio.

Taking into account the ratio $B_i : 2M_i : M = 1 : 2 : 1$ and the probabilities for the production of quarks of different flavours q_i , given by (1), we obtain $p/\pi^+ \simeq 0.21$ for $\lambda = 0$. We can easily get the p/π^+ ratio for an arbitrary λ : the decomposition of the ensembles $B_i(0)$, $M_i(0)$, $M(0)$ with respect to hadron states has been performed in Ref. [5] (see Appendix D, Tables D.1 and D.2). But, as was stressed above, this ratio is a weakly dependent function of λ : at $\lambda = 1$ we have $p/\pi^+ \simeq 0.20$.

B. Production of highly excited resonances and the Watson-Migdal factor

For quark combinatorics the saturation of $q\bar{q}$ and qqq states by real hadrons is of principal importance. The probability of saturation is defined by the coefficients $(\mu_L, \mu_L^{(i)})$ and $(\beta_L, \beta_L^{(i)})$ in (72). The main question is what contribution from high multiplets is important enough not to be negligible in the spectra.

Consider in more detail the production of mesons in the central region: $q\bar{q} \rightarrow M$. The central production of $q\bar{q}$ states is provided by the diagrams of Fig. 6 (loop diagram, Fig. 6a, and interactions of the produced quarks, Fig. 6b). The diagrams of the type of Fig. 6b for final state interactions lead to the relativistic Watson-Migdal factor. To estimate how many highly excited states are produced, we have to find out which states are determined by the $q\bar{q}$ system in the multiperipheral ladder.

The constructive element of the ladder is a process shown in Fig. 5b. In this process, as was stressed in Section 4, new $q\bar{q}$ pairs are created at relatively large separations (in hadronic scale), at $r \sim 1$ fm: these separations are just those in the $q\bar{q} \rightarrow M$ transitions. The orbital momenta of the $q\bar{q}$ system for this transition can be written as $L \sim kr$. For relative quark momenta $k \lesssim 0.6$ GeV/c, we have:

$$L \lesssim 3. \quad (75)$$

Relying on the behaviour of the Regge trajectory, one can understand, to what meson masses μ this relation corresponds. The trajectories for $q\bar{q}$ states are linear up to $\mu \sim 2.5$ GeV [33]:

$$\alpha(\mu^2) \simeq \alpha(0) + \alpha'(0)\mu^2, \quad (76)$$

the slope $\alpha'(0)$ is approximately equal $\alpha'(0) \simeq 0.8$ GeV $^{-2}$ and the intercept belongs to the interval $0.25 \lesssim \alpha(0) \lesssim 0.5$. Hence, for large μ , the estimation gives $\mu^2 \sim \alpha(\mu^2)/\alpha'(0)$; with $\alpha(M^2) \sim 3$, we have $\mu^2 \sim 4$ GeV 2 . So we conclude that in the multiperipheral ladder it would be natural to expect the production of $q\bar{q}$ mesons with masses

$$\mu \lesssim 2 \text{ GeV}. \quad (77)$$

It is instructive to write down the $q\bar{q}$ states which belong to this interval and saturate the expansions (72). The $q\bar{q}$ states are characterized by the orbital momentum L , the quark spin $S = 0, 1$ and the total momentum J ; one more characteristics of the $q\bar{q}$ state is the radial quantum number n . In the region $\mu \lesssim 2$ GeV the following $q\bar{q}$ multiplets $n^{2S+1}L_J$ with $n = 1$ are located [10,33]:

$$\begin{aligned} &1^1S_0, \quad 1^3S_1; \\ &1^1P_1, \quad 1^3P_J \quad (J = 0, 1, 2); \\ &1^1D_2, \quad 1^3D_J \quad (J = 1, 2, 3); \\ &1^1F_3, \quad 1^3F_J \quad (J = 2, 3, 4). \end{aligned} \quad (78)$$

As (75) tells us, all these states contribute significantly to the meson production.

The contribution of states with $n > 1$ is determined by the structure of the interaction of quarks in the final state, see Fig. 5b. For each partial wave the sum of diagrams with final state interaction is:

$$\frac{1}{1 - B(s_{q\bar{q}})} \Pi(s_{q\bar{q}}, s'_{q\bar{q}}) \frac{1}{1 - B^*(s'_{q\bar{q}})} , \quad (79)$$

where $1/(1 - B(s_{q\bar{q}}))$ is the relativistic Watson–Migdal factor:

$$B(s_{q\bar{q}}) = \int_{4m^2}^{\infty} \frac{ds}{\pi} \frac{N(s)\rho(s)}{s - s_{q\bar{q}}} = \text{Re } B(s_{q\bar{q}}) + iN(s_{q\bar{q}})\rho(s_{q\bar{q}}) . \quad (80)$$

Here the function $N(s)$ characterizes the interaction of quarks for given partial wave.

The cross section of $q\bar{q}$ pair production with invariant mass squared $s_{q\bar{q}}$ is determined by (79) at $s'_{q\bar{q}} = s_{q\bar{q}}$:

$$d\sigma\left(q\bar{q}(s_{q\bar{q}}) + X\right) \sim \Pi(s_{q\bar{q}}, s_{q\bar{q}}) \frac{1}{(1 - B(s_{q\bar{q}}))(1 - B^*(s_{q\bar{q}}))} . \quad (81)$$

It follows from quark–hadron duality that $d\sigma\left(q\bar{q}(s_{q\bar{q}}) + X\right)$ describes in the average the spectrum of produced resonance:

$$d\sigma\left(q\bar{q}(s_{q\bar{q}}) + X\right) \simeq d\sigma\left(\sum(\text{Resonances near } s_{q\bar{q}}) + X\right). \quad (82)$$

The averaging of the resonance production cross section is performed over a certain vicinity of $s_{q\bar{q}}$. In this way we see that the structure of the Watson–Migdal factor determines the rate of decrease of $d\sigma\left(q\bar{q}(s_{q\bar{q}}) + X\right)$ with the growth of the invariant mass as well as the quantitative contribution of the resonances with $n > 1$.

There are the following $q\bar{q}$ multiplets of the radial excitations in the region $\mu \lesssim 2$ GeV [33]:

$$\begin{aligned} n^1 S_0 , \quad n^3 S_1 \quad (n = 2, 3) ; \\ n^1 P_1 , \quad n^3 P_{0,1,2} \quad (n = 2) . \end{aligned} \quad (83)$$

The probability to produce these states is determined by the decrease of $d\sigma\left(q\bar{q}(s_{q\bar{q}}) + X\right)$, and by the Watson–Migdal factor in particular.

Summarizing, we definitely expect a considerable production of resonances belonging to $q\bar{q}$ multiplets with $n = 1$, see (78). With less definiteness we can judge upon the production of resonances with $n > 1$ presented in (83): if the Watson–Migdal factor suppresses strongly the contribution of large $s_{q\bar{q}}$, the production of multiplets is suppressed as well; but another situation is also plausible.

Only a small part of resonances belonging to the multiplets (78) and located at 1500 – 2000 MeV is included into the tables of [10]; a considerable number of resonances were discovered and identified only recently, see [33–36] and references therein. Moreover, numerous decay channels related to multiparticle states have not been identified yet. This makes the restoration procedure of the prompt probabilities on the basis of exclusion the known resonances [37–39] doubtful.

There is one more effect which makes the realization of the program of [37–39] questionable presently: the effect of the accumulation of widths of the overlapping resonances by one of them [40]. An identification of broad states with widths of the order of $\Gamma/2 \sim 400 - 600$ MeV in the mass region 1500 – 2000 MeV looks rather ambiguous at the present level of the experimental data, although the existence of such a type of states seems to be probable if we expect the existence of exotic mesons (glueballs and hybrids) in this mass region (see [40] for details).

VI. COHERENT PRODUCTION OF THE ω AND ρ^0 MESONS AT LARGE X

Indications on coherent phenomena in the hadronic Z^0 decays follow from the ratio ω/ρ^0 at $x \sim 1$, see Fig. 4f. In multiparticle processes, where the yields of ρ and ω occur without interference of flavour components, the ratio

$$\omega/\rho^0 = 1 \quad (84)$$

is valid.

Because of the approximate equality of masses of ρ and ω , the equation (84) is not violated by the decay of the highly excited resonances. The figure 4f demonstrates the validity of (84) at $x \sim 0.1 - 0.2$. However, at $x \sim 0.5 - 1.0$ the ratio ω/ρ^0 is definitely less than unity, thus unambiguously pointing to the interference of flavour components of the amplitudes $Z^0 \rightarrow u\bar{u}$ and $Z^0 \rightarrow d\bar{d}$.

Consider the production of ω and ρ in the quark jet. If the hadronization of quarks in jets $Z^0 \rightarrow u + X$ and $Z^0 \rightarrow d + X$ happens in a non-coherent way, the leading quark in the u -jet picks up an antiquark \bar{u} from the sea, giving rise to the transition $u\bar{u} \rightarrow (u\bar{u} + d\bar{d})/2 + (u\bar{u} - d\bar{d})/2 = \omega/\sqrt{2} + \rho^0/\sqrt{2}$. Likewise, in the d -jet $d\bar{d} \rightarrow (u\bar{u} + d\bar{d})/2 - (u\bar{u} - d\bar{d})/2 = \omega/\sqrt{2} - \rho^0/\sqrt{2}$. If there is no interference of u - and d - jets, the equation (84) is valid for each of them. But if the production amplitudes of ω and ρ do interfere, the equation (84) is violated. Let us consider the ratio ω/ρ^0 for such a case.

The amplitude of fragmentation production of u and d quarks is determined by the vertex of the transition $Z^0 \rightarrow q_i \bar{q}_i$ which has the following structure $[\bar{\psi}_i \gamma^\mu (g_V^i - g_A^i \gamma_5) \psi_i] Z_\mu$; for the u quark $g_A^{(u)} = 1/2$, $g_V^{(u)} = 1/2 - 4/3 \sin^2 \theta_w$ and for the d quark $g_A^{(d)} = -1/2$, $g_V^{(d)} = -1/2 + 2/3 \sin^2 \theta_w$. Therefore, for the axial-vector interaction we have the following transition:

$$\begin{aligned} A &\rightarrow 0.5 [u + (q\bar{q} - sea + \bar{u})] - 0.5 [d + (q\bar{q} - sea + \bar{d})] \\ &\rightarrow 0.5 [(u\bar{u} + X_{u\bar{u}}] - 0.5 [(d\bar{d} + X_{d\bar{d}}] . \end{aligned} \quad (85)$$

If $X_{u\bar{u}}$ and $X_{d\bar{d}}$ stand for the same state, $X_{u\bar{u}} = X_{d\bar{d}} \equiv X$, then

$$A \rightarrow \frac{1}{2}(u\bar{u} - d\bar{d}) + X = \sqrt{2}\omega + X . \quad (86)$$

The amplitude which is due to the vector interaction is

$$\begin{aligned} V &\rightarrow 0.19 [u + (q\bar{q} - sea + \bar{u})] - 0.35 [d + (q\bar{q} - sea + \bar{d})] \\ &\rightarrow 0.19 [(u\bar{u} + X_{u\bar{u}}] - 0.35 [(d\bar{d} + X_{d\bar{d}}] . \end{aligned} \quad (87)$$

With $X_{u\bar{u}} = X_{d\bar{d}}$ we have:

$$V \rightarrow \sqrt{2}(-0.16\omega + 0.54\rho^0) + X . \quad (88)$$

Therefore, for the axial-vector and vector interactions the ratios are:

$$\left(\frac{\omega}{\rho^0}\right)_{axial} = 0 , \quad \left(\frac{\omega}{\rho^0}\right)_{vector} = 8.8 \cdot 10^{-2} . \quad (89)$$

Hence, the coherent processes strongly suppress the production of ω meson compared to ρ^0 . In the experiment $\omega/\rho^0 \simeq 0.4$ at $x \sim 0.5 - 1$, that enables us to evaluate the contribution of coherent processes to be of the order of 50%.

VII. CONCLUSION

The rules of quark combinatorics are the consequence of the quark structure of hadrons, which directly reveals itself in the ratio $\rho_{prompt}/\pi_{prompt} = 3$. This equality is valid for the multiparticle production processes such as the hadronic Z^0 decays and high-energy hadron collisions.

The spectra observed in the multiparticle production processes are formed mainly due to the decay of highly excited resonances. In the meson sector states with masses up to 1500 – 2000 MeV contribute significantly; we can suppose that in the baryon sector it would be the contribution of states up to 2000 – 3000 MeV. The reconstruction of the spectra of highly excited resonances does not seem possible on the present level of knowledge. Therefore, one should investigate the prompt particle yields using jets with large x where the contribution of the resonance decay products is considerably suppressed.

The ratio $\rho^0/\pi^0 = 3$ observed in the hadronic Z^0 decay at $x \sim 0.5 - 0.8$ agrees with the predictions of quark combinatorics reasonably well.

The value p/π^+ is also in agreement with the quark combinatorial predictions at large x , thus revealing the small (about 25%) probability to meet the diquark loop in the chain of quark loops.

The peripheral production of new $q\bar{q}$ pairs in the multiparticle production processes allows us to introduce the suppression parameter for the production of strange and heavy flavour quarks. The suppression parameters are determined by the ratio of quark masses, their values agree with the experimental data.

In the central region, at $x \lesssim 0.2$, the experiment gives us $\omega/\rho^0 \simeq 1$ that also agrees with the quark combinatorial rules. However, at $x > 0.5$ the experimental data definitely tell us that $\omega/\rho^0 < 1$ which is an indication to the interference of flavour amplitudes with the fragmentation production of u and d quarks: the signs of flavour amplitudes favour $\omega/\rho^0 < 1$.

As a conclusion, we can state that the predictions of quark combinatorics for hadronic decays of the Z^0 boson agree reasonably well with the experimental data.

ACKNOWLEDGEMENT

The authors are deeply indebted to L.G. Dakhno for many useful discussions. The paper was partly supported by RFBR grant 98-02-17236.

APPENDIX A: V/P RATIO IN THE HIGH-ENERGY HADRON-HADRON COLLISIONS

We demonstrate here that the ratio $V_{prompt}/P_{prompt} = 3$ is not specific for the decay processes — it is inherent in the hadronic multiple production processes as well.

We consider the meson central production cross section, which is governed by the two-pomeron diagram as is shown in Fig. 7a. The probability of the meson production is determined by the structure of a pomeron ladder; here we use a QCD-motivated pomeron based on the pQCD pomeron of [16]. In [16] the pomeron was constructed inserting the running coupling constant and soft interaction boundary condition. The pomeron found under these constraints, Lipatov's pomeron [16], has an infinite set of poles in the j -plane; it is a suitable object for using it as a guide in the analysis of the soft interaction region. Such an extension of Lipatov's pomeron into the soft region has been already used in [41]; below we follow the results of [41].

The gluon ladder which responds to Lipatov's pomeron is shown in Fig. 7b. For the description of soft interactions the quark loops can be incorporated into the gluon ladder since, according to the rules of $1/N$ expansion [17], the quark loops do not cause additional smallness. The cutting of quark loops (see Fig. 7c) provides the diagram which corresponds to the inclusive production cross section of the $q\bar{q}$ pair i.e. the production of meson states. In this sense the diagram of Fig. 7c is re-drawn as Fig. 7d: the quark-pomeron vertex is defined by the interaction of two reggeized gluons with a quark. The spin structure of such a vertex can be easily calculated (see [41], Appendix C) using the analysis of the leading- s terms in reggeon kinematics (large s and small t) for the vertex *vector particle + fermion* [42].

In the leading terms of the $1/N$ expansion there exist diagrams of the type of Fig. 7e in which the gluons of the upper (or lower) pomeron interacts with two quarks simultaneously (generally, these diagrams can be presented as Fig. 7f). As was shown in [41], the sum of all these contributions (Figs. 7d, 7e etc.) results in the colour screening effect: the quark loop amplitude is nearly zero for the mentioned quark configurations at $r_{q\bar{q}} \lesssim 0.2$ fm (the existence of the colour screening effects in hadron production processes was emphasized long ago [43,44]).

The colour screening effect for the quark loop diagram in the pomeron ladder [41] allows us to restrict the calculations of V_{prompt}/P_{prompt} to the process of Fig. 7a, because this diagram is responsible for the main effect at large $q\bar{q}$ separations, $r_{q\bar{q}} \gtrsim 0.2$ fm.

The loop diagram of Fig. 7a is defined by the formula which is quite similar to (8) — only the spin factors are substituted as follows: $S_\pi \rightarrow S_\pi^{(P)}$ and $S_\rho \rightarrow S_\rho^{(P)}$, that is due to the accounting for vertices $P_{q\bar{q}}$. The spin factors $S_\pi^{(P)}$ and $S_\rho^{(P)}$ read:

$$\begin{aligned} S_\pi^{(P)} &= -\text{Sp} \left(i\gamma_5(\hat{k}_1 + m)\hat{n}_+(\hat{k}_1 + m)i\gamma_5(-\hat{k}_2 + m)(-\hat{n}_-)(-\hat{k}_2 + m) \right) \\ S_\rho^{(P)} &= -\text{Sp} \left(\gamma_\alpha^\perp(\hat{k}_1 + m)\hat{n}_+(\hat{k}_1 + m)\gamma_\alpha^\perp(-\hat{k}_2 + m)(-\hat{n}_-)(-\hat{k}_2 + m) \right) . \end{aligned} \quad (90)$$

Here \hat{n}_+ is the quark–pomeron vertex (the coupling to the upper pomeron in Fig. 7a) and $(-\hat{n}_-)$ is the antiquark–pomeron vertex (the coupling to the lower pomeron); we have also taken into account that pomerons in the diagram of Fig. 7a for the inclusive cross section carry zero momenta.

If the upper pomeron in the graph of Fig. 7a moves along the z -axis with momentum $p_A = (p_0, 0, p_z) \simeq (p_z, 0, p_z)$, while the lower one moves in opposite direction, we have

$$n_- = (1, 0, -1), \quad n_+ = (1, 0, 1). \quad (91)$$

As in Section 2, the loop diagram has been calculated in terms of the spectral integration; because of that $k_1^2 = k_2^2 = m^2$. After the operators \hat{n}_+ and \hat{n}_- have been commutated with \hat{k}_1 and \hat{k}_2 , we have:

$$\begin{aligned} S_\pi^{(P)} &= -\text{Sp} \left(i\gamma_5(\hat{k}_1 + m)i\gamma_5(-\hat{k}_2 + m) \right) 4(n_+k_1)(n_-k_2) \\ S_\rho^{(P)} &= -\text{Sp} \left(\gamma_\alpha^\perp(\hat{k}_1 + m)\gamma_\alpha^\perp(-\hat{k}_2 + m) \right) 4(n_+k_1)(n_-k_2) \end{aligned} \quad (92)$$

Up to a common factor, $S_\pi^{(P)}$ and $S_\rho^{(P)}$ coincide with the normalizing spin factors of the pion and ρ -meson wave functions given by (24) and (29):

$$\begin{aligned} S_\pi^{(P)} &= 4(n_+k_1)(n_-k_2)S_\pi^{(wf)} \\ S_\rho^{(P)} &= 4(n_+k_1)(n_-k_2)3S_\rho^{(wf)}. \end{aligned} \quad (93)$$

This equation demonstrates that the two–pomeron diagram of Fig. 7a which defines the inclusive production cross section of ρ and π in the central region of hadron–hadron collisions gives us $\rho_{\text{prompt}}/\pi_{\text{prompt}} = 3$.

APPENDIX B: SPIN FACTORS FOR THE FRAGMENTATION PRODUCTION

Below the explicit expressions for $S_P^{(fr)}/S_P^{(wf)}$ and $S_V^{(fr)}/S_V^{(wf)}$ are given for the processes $Z^0 \rightarrow b\bar{b} \rightarrow B + X$ and $Z^0 \rightarrow b\bar{b} \rightarrow B^* + X$.

For the pseudoscalar particle we have:

$$\frac{S_P^{(fr)}}{S_P^{(wf)}} = A_1 + R^2 A_2, \quad (94)$$

where

$$\begin{aligned} A_1 &= ((m_b - m)^2 - s')(M^2 + 2m_b^2) + ((m_b - m)^2 - s)(M'^2 + 2m_b^2), \\ A_2 &= M^2 \left(1 - \frac{m_b^2}{M'^2} \right) ((m_b - m)^2 - s') + M'^2 \left(1 - \frac{m_b^2}{M^2} \right) ((m_b - m)^2 - s) \\ &\quad - 3m_b^2 ((m_b - m)^2 - s') - 3m_b^2 ((m_b - m)^2 - s); \end{aligned} \quad (95)$$

and for the fragmentation production of the vector particle:

$$\begin{aligned} \frac{S_V^{(fr)}}{S_V^{(wf)}} &= \frac{M^2}{ss'}A_3 + \frac{M'^2}{ss'}A_4 + \frac{2m^2}{ss'}(A_3 + A_4) \\ &\quad + \frac{R^2}{M'^2M^2s's} (M^4(M'^2 - m_b^2)A_3 + M'^4(M^2 - m_b^2)A_4 - 3M'^2M^2m_b^2(A_3 + A_4)). \end{aligned} \quad (96)$$

Here

$$\begin{aligned} A_3 &= (s + s')(m_b^2 - m^2)^2 + ss'(3m^2 - m_b^2 - 10m_b m - 4s') \\ &\quad + s'^2(3m_b^2 - 2m_b m - m^2), \\ A_4 &= (s + s')(m_b^2 - m^2)^2 + ss'(3m^2 - m_b^2 - 10m_b m - 4s) \\ &\quad + s^2(3m_b^2 - 2m_b m - m^2). \end{aligned} \quad (97)$$

- [1] V.V. Anisovich and V.M. Shekhter, Nucl. Phys. **B55**, 455 (1973).
- [2] J.D. Bjorken and G.E. Farrar, Phys. Rev. **D9**, 1449 (1974).
- [3] S.T. Butler and C.A. Pearson, Phys. Rev. Lett., **7**, 69 (1961);
A. Schwarzschild and C. Zupancic, Phys. Rev. **129**, 854 (1961);
J. Randrup and S.E. Koonin, Nucl. Phys. **A356**, 223 (1981);
D.H.E. Gross et al. Z. Phys. **A309**, 41 (1982).
- [4] K.M. Watson, Phys. Rev. **88**, 1163 (1952);
A.B. Migdal, ZETF **28**, 10 (1955).
- [5] V.V. Anisovich, M.N. Kobrinsky, J. Nyiri and Yu.M. Shabelski, "Quark Model and High Energy Collisions", World Scientific, Singapore, 1985.
- [6] M.A. Voloshin, Yu.P. Nikitin and P.I. Porfirov, Sov. J. Nucl. Phys. **35**, 586 (1982).
- [7] S.S. Gershtein, A.K. Likhoded and Yu.D. Prokoshkin, Z. Phys. **C24**, 305 (1984).
- [8] C. Amsler and F.E. Close, Phys. Lett. **B353**, 385 (1995); *ibid*, Phys. Rev. **D53**, 295 (1996).
- [9] V.V. Anisovich, Phys. Lett. **B364**, 195 (1995);
V.V. Anisovich, Yu.D. Prokoshkin and A.V. Sarantsev, Phys. Lett. **B382**, 429 (1996);
A.V. Anisovich and A.V. Sarantsev, Phys. Lett. **B413**, 137 (1997);
V.V. Anisovich, V.A. Nikonov and L. Montanet, Phys. Lett. **B480**, 19 (2000).
- [10] Particle Data Group, C. Caso et al., Eur. Phys. J. **C3**, 1 (1998).
- [11] ALEPH Coll., R. Barate et al., Phys. Rep. **294**, 1 (1998).
- [12] L3 Coll., M. Acciarri et al., Phys. Lett. **B393**, 465 (1997); *ibid*, **B407**, 389 (1997).
- [13] DELPHI Coll., P. Abreu et al., Phys. Lett. **B475**, 429 (2000); *ibid*, **B449**, 364 (1999).
- [14] OPAL Coll., K. Ackerstaff et al., Eur. Phys. J. **C4**, 19 (1998); *ibid*, Eur. Phys. J. **C5**, 411 (1998).
- [15] E.A. Kuraev, L.N. Lipatov and V.S. Fadin, Sov. Phys. JETP **44**, 443 (1976);
Ya.Ya. Balitsky and L.N. Lipatov, Sov. J. Nucl. Phys. **28**, 882 (1978).
- [16] L.N. Lipatov, Sov. Phys. JETP **63**, 904 (1986)
- [17] G. t'Hooft, Nucl. Phys. **B72**, 461 (1974);
G. Veneziano, Nucl. Phys. **B117**, 519 (1976).
- [18] V.V. Anisovich, "Strong Interaction Processes at High Energies and the Quark-Parton Model", in *Proceedings of the 9th PNPI Winter School* **3**, 1 (1974).
- [19] V.N. Gribov, Eur. Phys. J. **C10** 71 (1999), hep-ph/9807224; Eur. Phys. J. **C10** 91 (1999), hep-ph/9902279.
- [20] T. Barnes, "Phenomenology of Light Quarks", in *Hadron Spectroscopy*, AIP Conference Proceedings 432, EDS. S.-U. Chung and H.J. Willutzki, Woodbury, NY (1998).
- [21] V.V. Anisovich, M.G. Huber, M.N. Kobrinsky and B.Ch. Metsch, Phys. Rev. **D42**, 3045 (1990);
V.V. Anisovich and B.Ch. Metsch, Phys. Rev. **D46**, 3195 (1992).
- [22] ALEPH Coll., D. Busculic et al., Z. Phys. **C69**, 393 (1996).
- [23] DELPHI Coll., P. Abreu et al., Z. Phys. **C68**, 353 (1995).
- [24] L3 Coll., M. Acciarri et al., Phys. Lett. **B345**, 353 (1995).
- [25] OPAL Coll., K. Ackerstaff et al., Z. Phys. **C74**, 413 (1997).
- [26] ALEPH Coll., R. Barate et al. "Study of charm production in Z decay", preprint CERN/EP/99-94.
- [27] DELPHI Coll., P. Abreu et al., "Measurement of the Z partial decays into $c\bar{c}$ and multiplicity of charm quarks per b decay", preprint CERN/EP/99-66.
- [28] OPAL Coll., K. Ackerstaff et al., Eur. Phys. J. **C5**, 1 (1998).
- [29] V.V. Anisovich, D.I. Melikhov and V.A. Nikonov, Phys. Rev. **D52**, 5295 (1995); *ibid* **D55**, 2918, (1997).
- [30] V.V. Anisovich, D.I. Melikhov, B.Ch. Metsch and H.R. Petry, Nucl. Phys. **A563**, 549 (1993).
- [31] D.B. Leinweber et al., Phys. Rev. **D58**: 031501 (1998).
- [32] K. Peters and E. Klempt, Phys. Lett. **B352**, 467 (1995).
- [33] A.V. Anisovich, V.V. Anisovich and A.V. Sarantsev, "Systematics of $q\bar{q}$ states in the (n, M^2) and (J, M^2) planes", hep-ph/0003113, Phys. Rev. D, in press.
- [34] C.A. Baker, C.J. Batty, P. Blüm et al., Phys. Lett. **B449**, 114 (1999).
- [35] D. Barberis, F.G. Binon, F.E. Close et al., WA 102 Coll., "A study of the $f_0(980)$, $f_0(1370)$, $f_0(1500)$, $f_0(2000)$, and $f_2(1950)$ observed in the centrally produced 4π states", hep-ex/0001017 (2000).
- [36] A.V. Anisovich, C.A. Baker, C.J. Batty et al., Phys. Lett. **B452**, 187 (1999); *ibid*, **B452**, 173 (1999); *ibid*, **B452**, 180 (1999); Nucl. Phys. **A651**, 253 (1999).
- [37] Yi-Jin Pei, Z. Phys. **C72**, 39 (1996).
- [38] P.V. Chliapnikov, Phys. Lett. **B462**, 341 (1999).
- [39] V. Uvarov, Proc. of the XVth Particle and Nuclei Int. Conference, Uppsala, Eds. G. Fäldt et al., 1999.
- [40] V.V. Anisovich, D.V. Bugg and A.V. Sarantsev, Phys. Rev. **D58**:111503 (1998);
A.V. Anisovich, V.V. Anisovich and A.V. Sarantsev, Z. Phys. **A357**, 173 (1997).
- [41] L.G. Dakhno and V.A. Nukonov, Eur. Phys. J. **A5**, 209 (1999).
- [42] V.N. Gribov, L.N. Lipatov and G.V. Frolov, Sov. J. Nucl. Phys. **12** 543 (1971).

- [43] A.H. Mueller, in Proceedings of the 17th Rencontre de Moriond: Elementary Hadronic Processes and New Spectroscopy, Les Arcs, Ed. J. Tran Than Van, Editions Frontieres, Gif-sur-Yvette, 1982.
- [44] S.J. Brodsky, in Multiparticle Dynamics 1982, Proceedings of the 13th International Symposium, Volendam, Eds. W. Metzger, E.W. Kittel and A. Stergiou, World Scientific, Singapore, 1983.

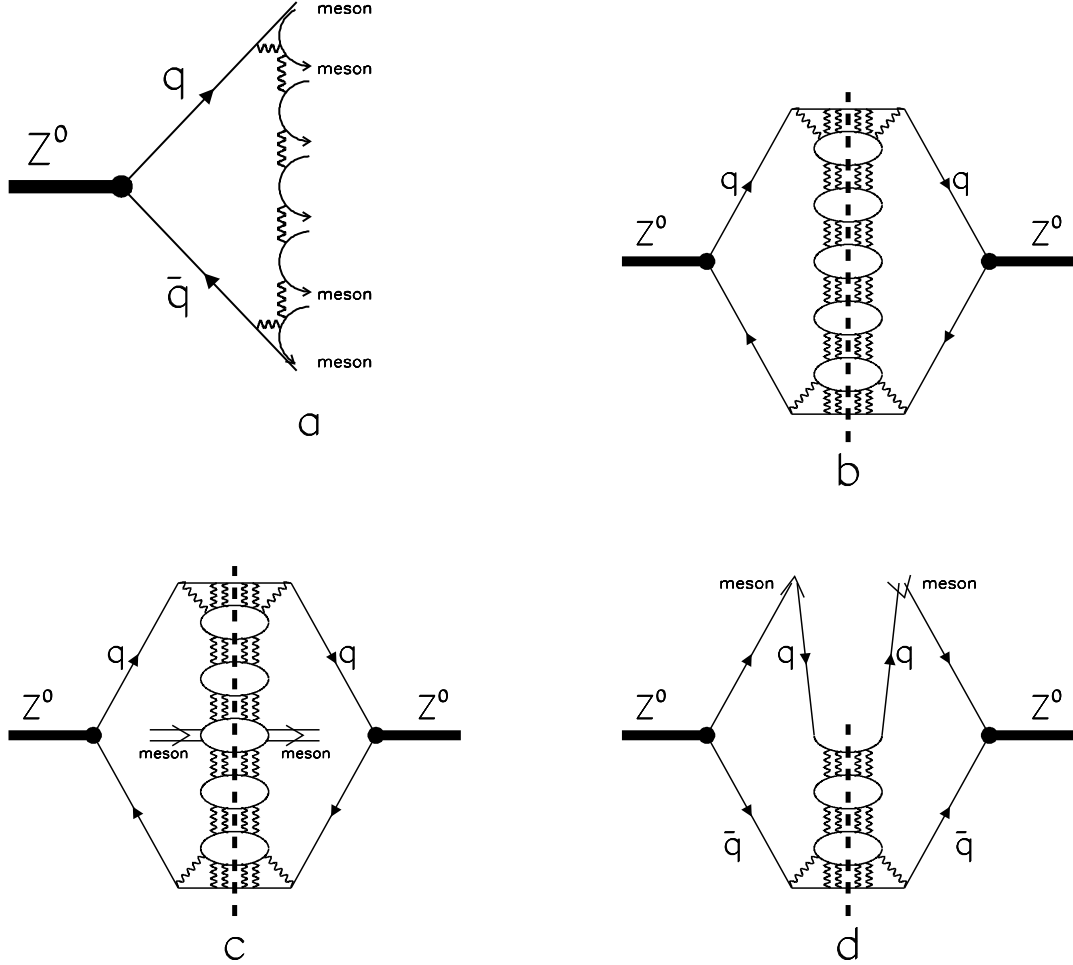


FIG. 1. Hadronic decay of Z^0 meson. a) Multiperipheral ladder which provides the transfer of colour from quark to antiquark. b) Self-energy diagram; the cutting along hadronic states (dashed line) determines the hadronic cross section. c) Diagram for the inclusive meson production cross section in the central region, $d\sigma(Z^0 \rightarrow meson + X)/dx$ at $x \sim 0$. d) Diagram for the inclusive meson production cross section in the fragmentation region at $x \sim 0.2 - 1$.

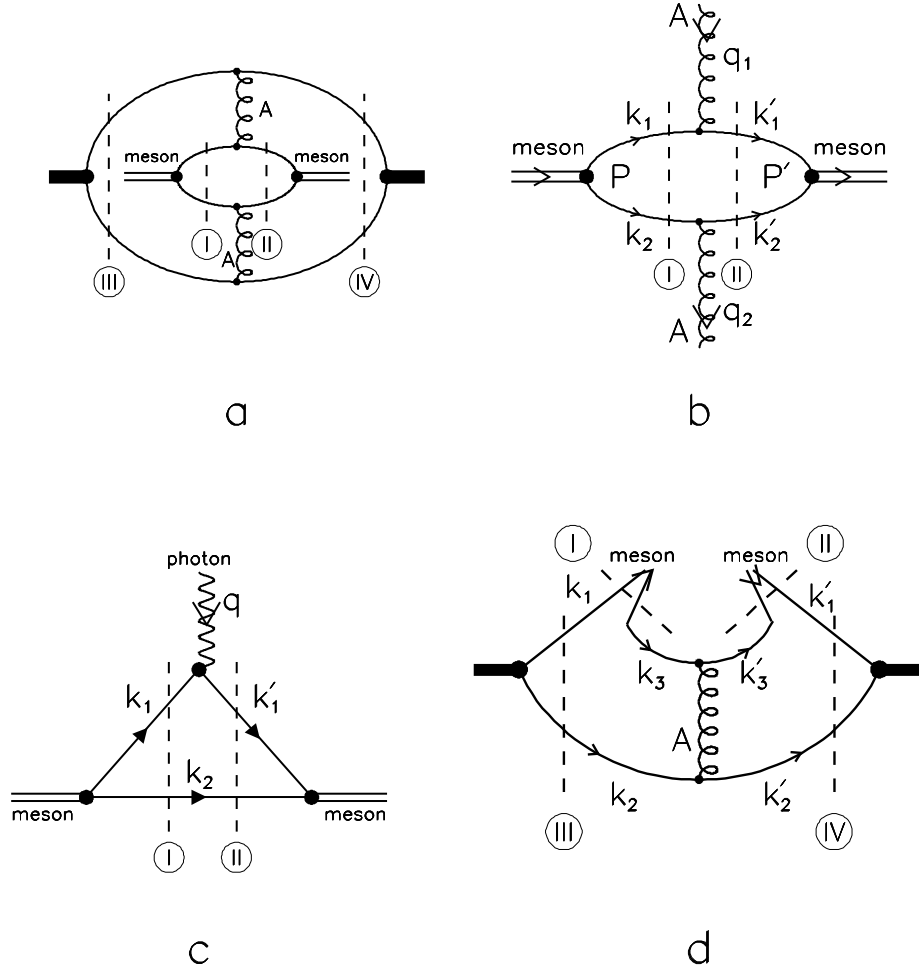


FIG. 2. a,b) Production blocks for meson in the central region; the dashed lines show the cuttings of diagrams in the spectral integral. c) Form factor diagram determining the meson wave function. d) The cuttings of the diagram for the inclusive meson production cross section in the fragmentation region.

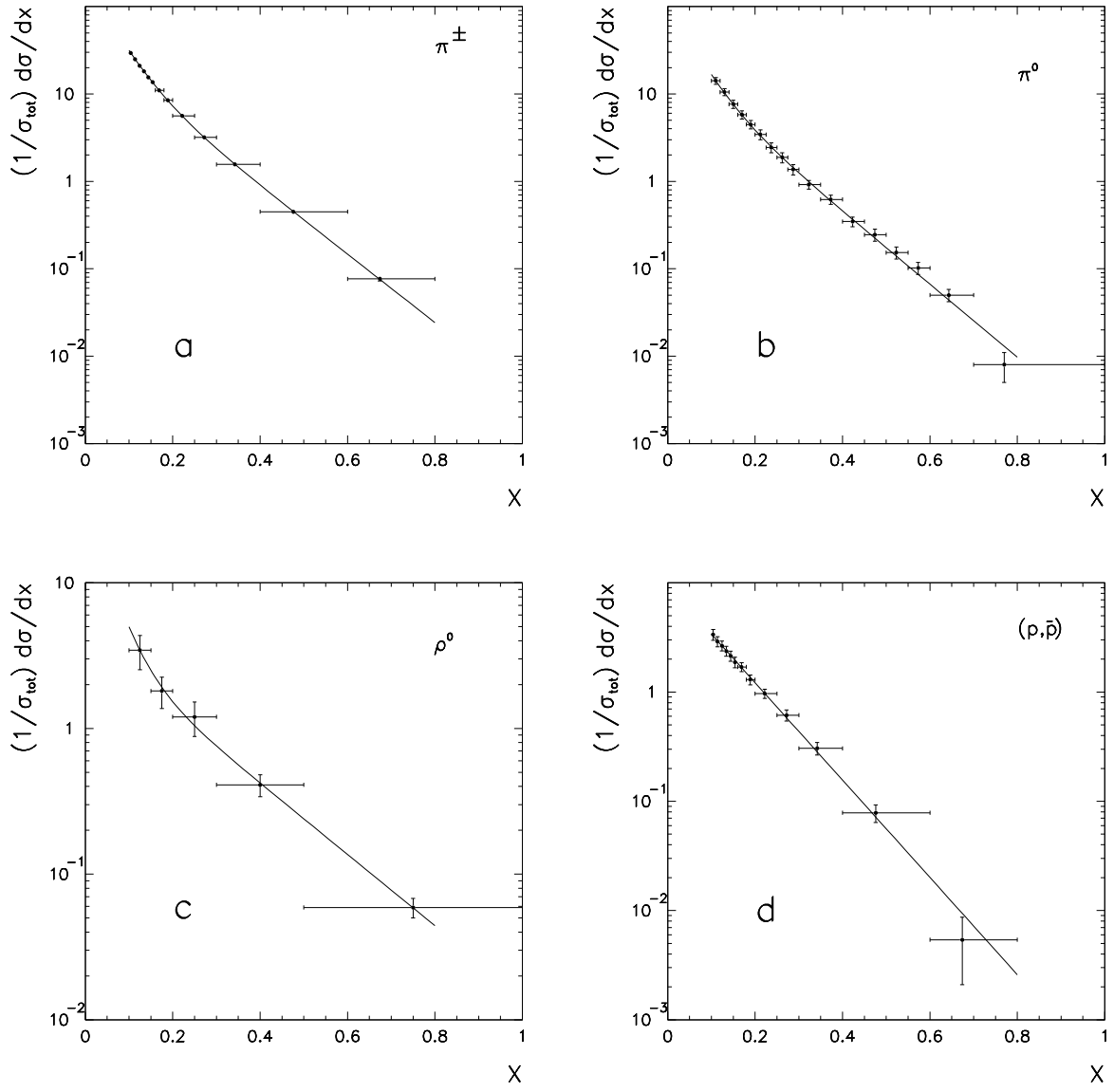


FIG. 3. The spectra $(1/\sigma_{\text{hadron}}) d\sigma_{Z^0 \rightarrow \text{meson}+X}/dx$ [11] for a) π^\pm , b) π^0 , c) ρ^0 and d) (p, \bar{p}) and their fit by exponential functions $\Sigma C_i \exp(-b_i x)$ [11].

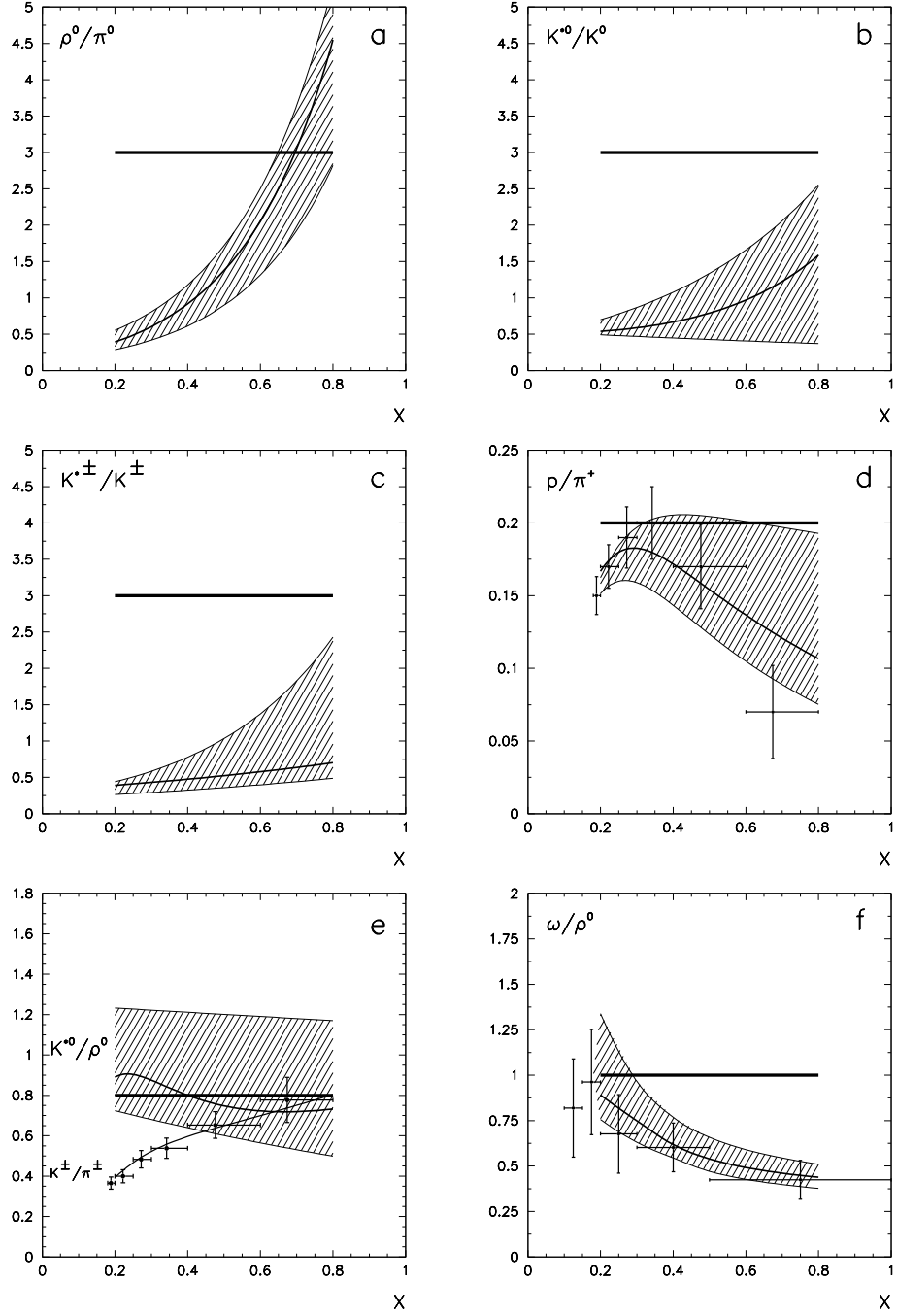


FIG. 4. Ratios ρ^0/π^0 (a), K^{*0}/K^0 (b), $K^{*\pm}/K^\pm$ (c), p/π^+ (d), K^{*0}/ρ^0 and K^\pm/π^\pm (e), ω/ρ^0 (f) obtained from the exponential fit to ALEPH data [11] (shaded areas). Solid lines stand for the predictions of quark combinatorics rules. In Figs. 4d, 4e, 4f the ratios p/π^+ , K^\pm/π^\pm and ω/ρ^0 which are obtained using a histogram description of the spectra [11] are also shown.

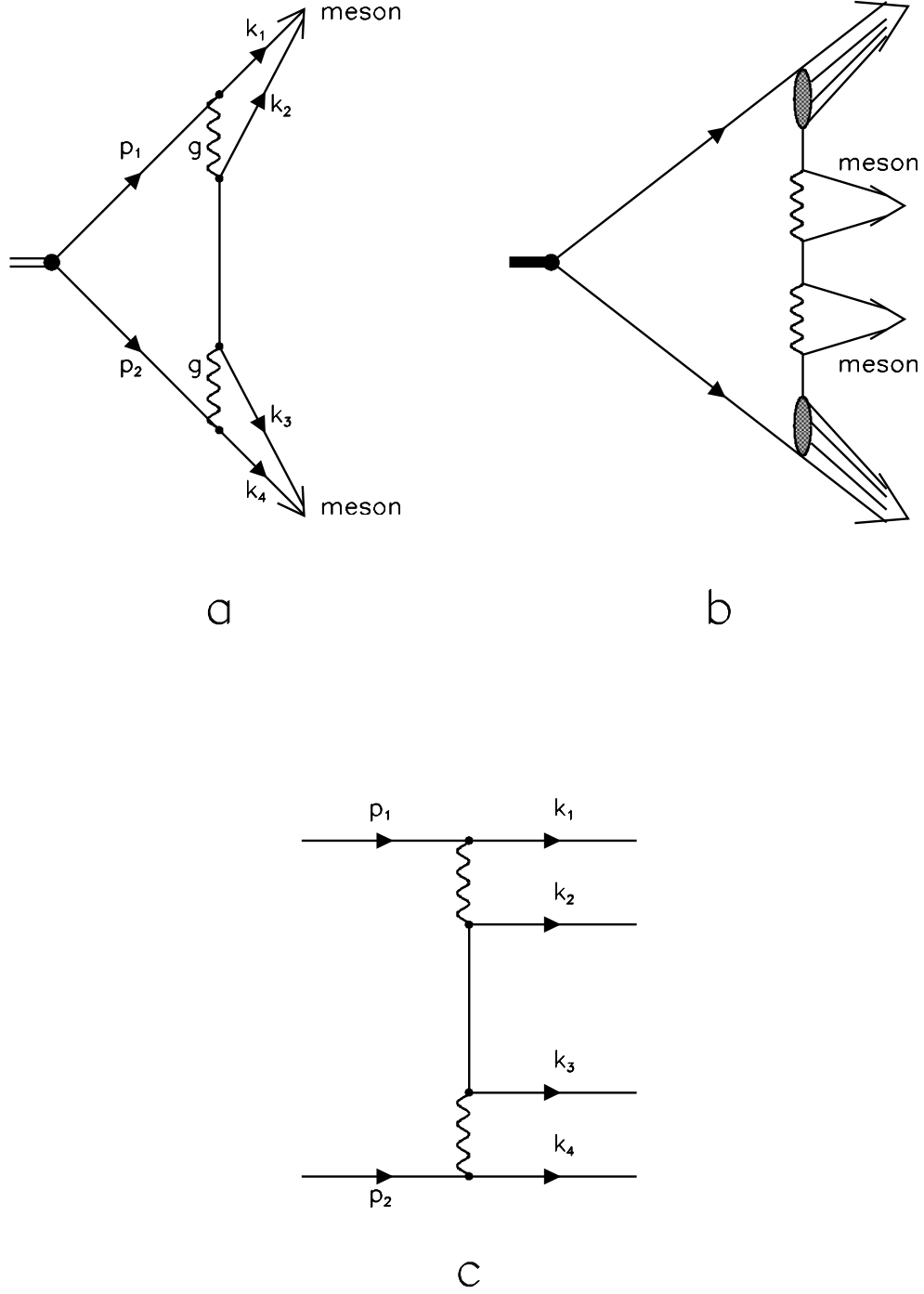


FIG. 5. a) Meson decay diagram. b) The transition $q\bar{q} \rightarrow meson + meson$ as the constructive element of the multiperipheral chain in the hadronic Z^0 decay. c) Diagram for the peripheral production of the new $q\bar{q}$ pair.

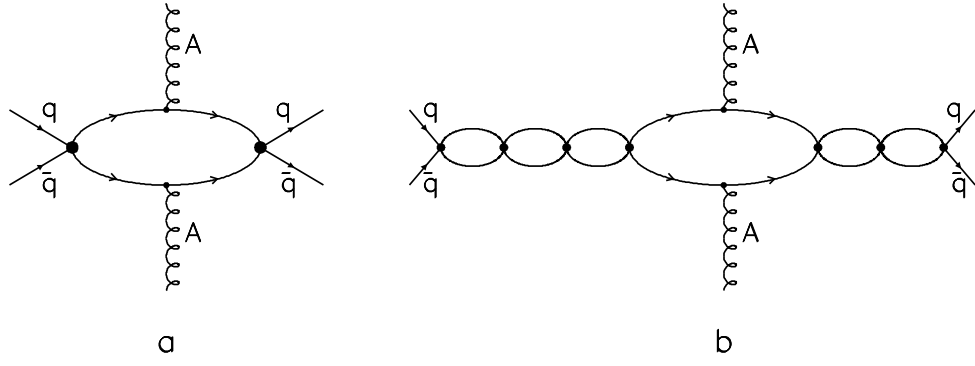


FIG. 6. Diagrams for the central production of $q\bar{q}$ pair. The set of loop diagrams responsible for the Watson–Migdal factor.

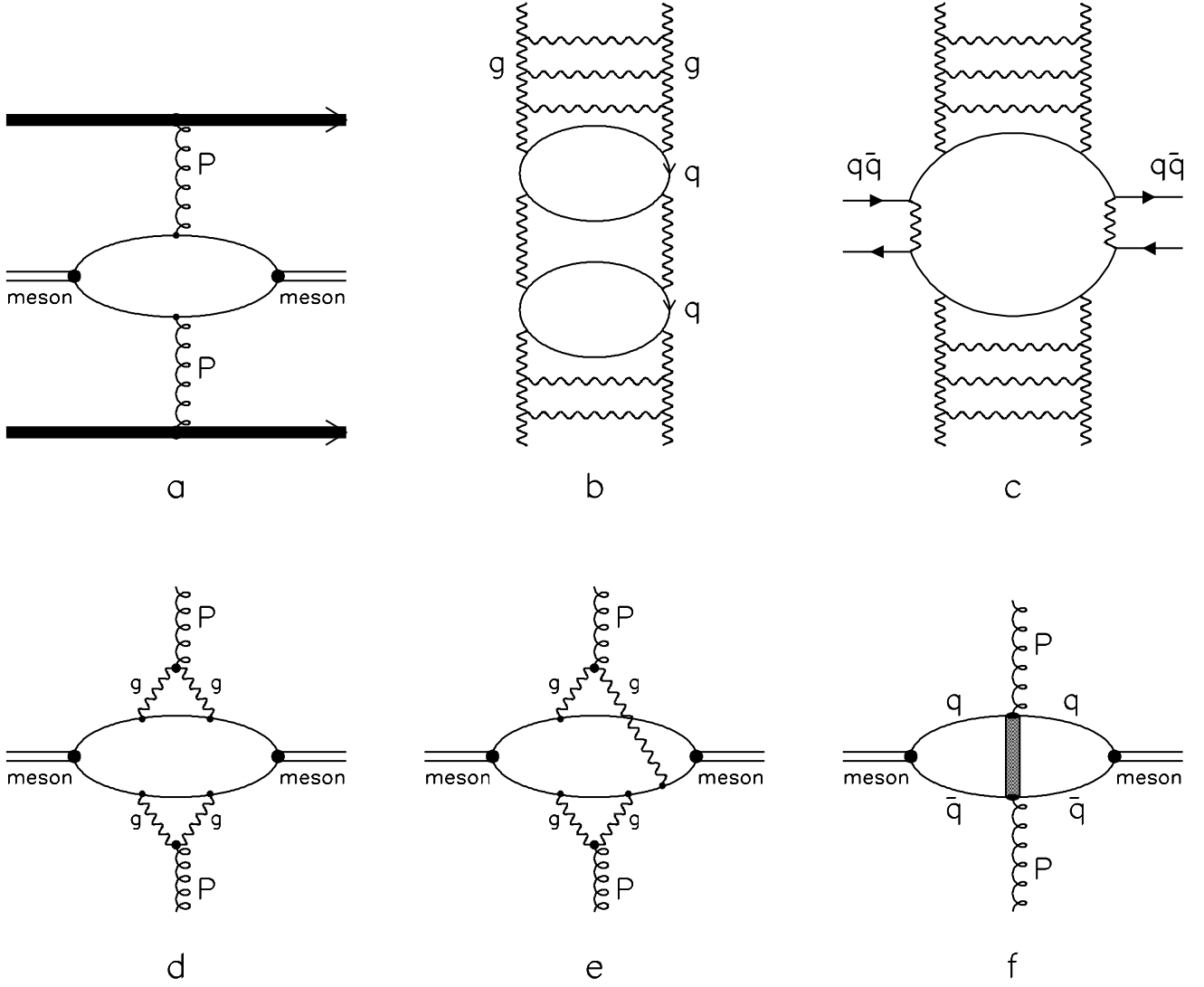
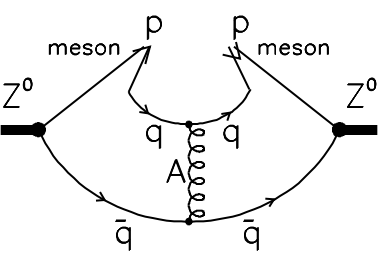
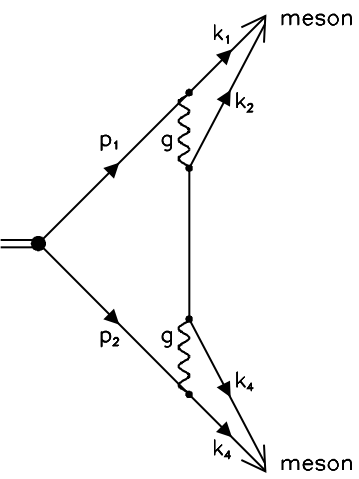


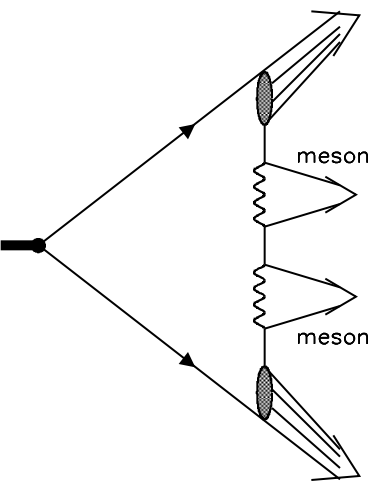
FIG. 7. Diagrams for meson production in the central region in high energy hadron-hadron collisions.



e



a



b